Developing hydrogeophysics for critical zone studies, importance of heterogeneities and processes at the mesoscopic scale

—

Habilitation thesis (HDR)
Defended in Sorbonne Université, Paris
January 17, 2020

—

Damien Jougnot

Foreword

This document is a dissertation to obtain the HDR (Habilitation à Diriger la Recherche), a french diploma for research and student supervision. I defended this degree on January 17 2020, at Sorbonne University, in Paris, in front of a Jury composed of Colette Siriex, Jean-François Girard, Frédéric Nguyen, Linda Luquot, and Valérie Plagne (president).

The present manuscript synthesizes the research that I have been conducting during the last ten years (i.e., since the my PhD defense): during 5 years at University of Lausanne as a post-doc in the group of Niklas Linde and during 5 years at UMR 7619 METIS, Sorbonne Université, as a CNRS researcher. These investigations are the result of a collective work in close interaction with PhD students, postdocs, and researchers in my labs but also abroad. Indeed, in addition to my host institutions, I had the chance build up a network of fruitful national and international collaborations (Argentina, Belgium, Denmark, France, Germany, United States, Spain, Switzerland). More information about my research and links to my publications can be found on my website: `https://sites.google.com/site/damienjougnot/`

Abstract

The critical zone is the thin outer layer supporting life on earth. It is a compartment in which many complex and coupled bio-chemico-physical processes take place. Characterizing and monitoring these processes is of utmost importance to understand and protect the critical zone. Geophysical methods are very appropriate tools to study them in situ and non-intrusively thanks to the sensitivity of measurable physical parameters to properties of interest. However, the critical zone is also a very heterogeneous medium at different scales and the quantitative use of geophysics rely on our capability to take them into account effectively. In this manuscript I present the various works that I conducted during the last ten years to better use hydrogeophysical methods by taking heterogeneities into account: from theoretical petrophysical model developments to laboratory experiments and in situ monitoring in critical zone observatories. After presenting the geophysical methods I have been using, I define the concept of mesoscopic scale heterogeneities, that is: larger than the pore scale but smaller than the resolution of the considered geophysical method. The first heterogeneities that I present are related to the pore size distribution and its impact on the water saturation, flow and solute transport properties. The second heterogeneities that I study are the presence of fractures and fracture networks in porous media. The final kind of heterogeneities that I am considering are induced by local biogeochemical reactions and their impact on geophysical signals. These new advances and on-going research projects pave the way to a more quantitative and more integrated use of geophysics to study the critical zone in its true complexity.

Keywords: Critical zone, Hydrogeophysics, Heterogeneous media, Petrophysics, Up-scaling

Résumé

La zone critique est la fine pellicule externe qui permet la vie sur terre. C'est un compartiment dans lequel ont lieu de nombreux processus couplés bio-chimio-physiques. La caractérisation et le suivi de ces processus sont d'une importance cruciale pour comprendre et protéger la zone critique. Les méthodes géophysiques sont des outils tout particulièrement adaptés pour étudier ces processus in situ et de façon non-intrusive grace à la sensibilité des mesurables physiques aux propriétés d'intérêt de la zone critique. Toutefois, la zone critique est un milieu très fortement hétérogène aux différentes échelles et l'utilisation quantitative de la géophysique dépend de notre capacité à les prendre en compte efficacement. Dans ce manuscrit, je présente les différents travaux que j'ai menés durant les dix dernières années pour une meilleur utilisation de l'hydrogéophysique en prenant en comptes ces hétérogénéités: du développement de modèles pétrophysiques au expériences de laboratoire et aux suivi in situ dans des observatoires de la zone critique. Après une brêve présentation des méthodes géophysique que j'ai utilisées, je définis le concept d'hétérogénéités à l'échelle mésoscopique, c'est à dire plus grande que l'échelle porale mais inférieure à la résolution de la méthode géophysique considérée. Les premières hétérogénéités que je présente sont liées à la distribution de taille des pores dans le milieu et son impact sur la saturation en eau, le flux d'eau et le transport de solutés. La deuxième sorte d'hétérogénéités que j'étudie est la présences de fractures en milieu poreux et de réseaux de fractures. Le dernier genre d'hétérogénéité que je considère est induit par des réactions biogéochimiques à l'échelle locale et leur impact sur les signaux géophysiques. Ces nouvelles avancées et les projets de recherche que je mène actuellement ouvrent la voie à une utilisation plus quantitative et intégrée de la géophysique pour l'étude de la zone critique dans toute sa complexité.

Mots clés: Zone critique, Hydrogéophysique, Milieux hétérogènes, Pétrophysique, Changement d'échelle

Contents

List of Figures

Chapter 1

Introduction

The **Critical Zone** has first been defined by the US National Research Council in 2001 as the first research opportunity for the near future.

> *"The **Critical Zone**: [an] heterogeneous, near surface environment in which complex interactions involving rock, soil, water, air, and living organisms regulate the natural habitat and determine the availability of life-sustaining resources."* (NRC, 2001)

And a shorter definition of the critical zone could be the earth skin: "*from the top of the canopy down to the base of the groundwater zone*". Since then, the critical zone has been the subject of an increasing number of scientific studies and publications (Fig. 1.1).

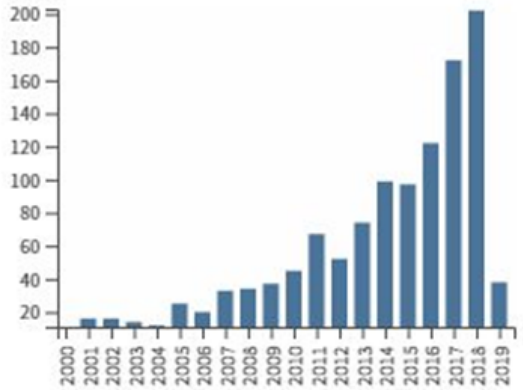

Figure 1.1: Evolution of the number of publications with the topic "Critical Zone" in Web of Science (search results obtained on March 11, 2019).

Critical zone studies are truly trans-disciplinary by nature as they cross so many scientific research areas in geosciences. The "critical" importance of this zone to human societies and life on earth in general is generating researches of more philosophical nature, such as Arènes et al. (2018) recently proposed to replace the critical zone "at the center of the attention" given the various environmental issues that the human species will have to face in the near future (Fig. 1.2).

Studying the critical zone Better understanding the critical zone is also a matter of research strategies in which overlap observation, modeling, and process studies in controlled environments. Critical zone observatories and networks exist in different countries across the world. In France the study of the critical zone is mainly done through two main initiatives: OZCAR (Observatoires de la Zone Critique Application et Recherche or Critical Zone Observatories - Application and Research, see `https://www.ozcar-ri.org/`) and CRITEX (challenging equipment for the temporal and

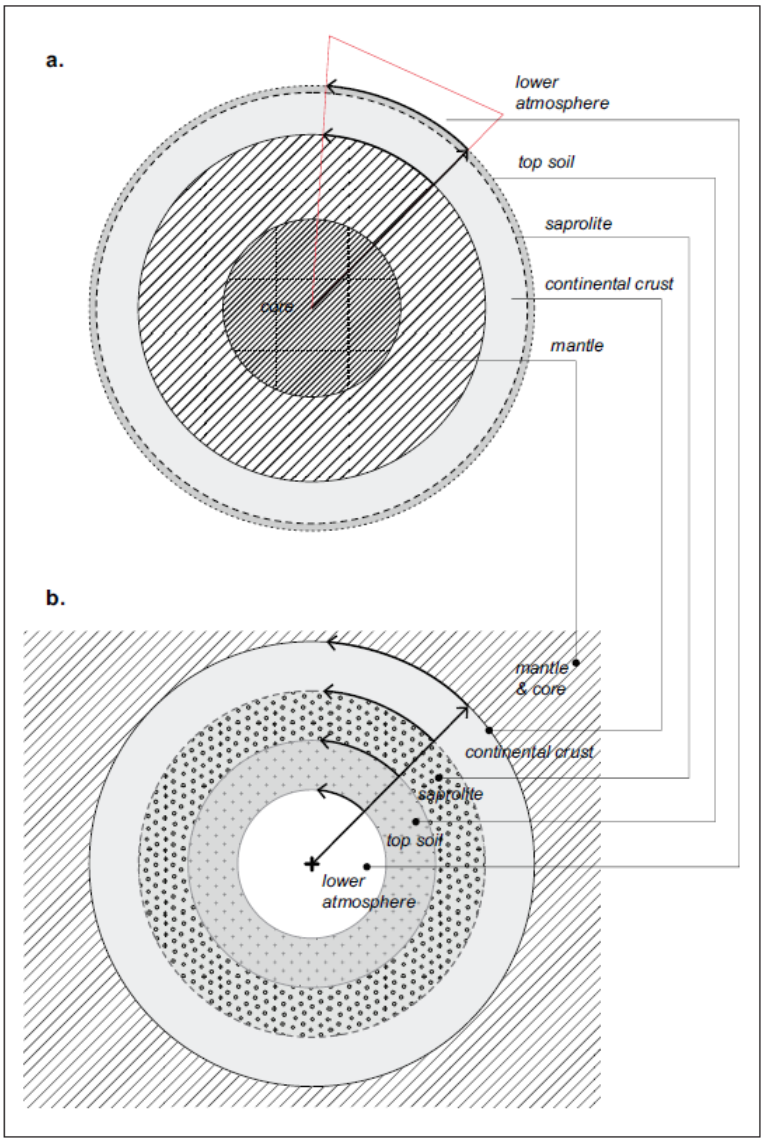

Figure 1.2: Replacing the critical zone at the center of the attention: (a) classical view of the globe and (b) anamorphosis that places the layers that are really critical for life on Earth in the center (Arènes et al., 2018).

spatial exploration of the critical zone at the catchment scale, see `https://www.critex.fr/`) (Gaillardet et al., 2018).

The three main scientific research orientations and open questions for critical zone studies through the OZCAR test site network are:

- **Dynamic architecture of the Critical Zone**: What is the vertical and lateral extent of the Critical Zone? What are the residence and exposure times of water and matter in the different compartments? What are the critical zone interfaces? what are the important critical zone interfaces? What is the role of biota in the Critical Zone?

- **Biogeochemical cycles, sediment and/or contaminant propagation through the critical zone from highlands to sea**: Can we better quantify budgets of mass and energy across our critical zone observatories? How high frequency sampling can help deciphering critical zone functioning? What is the functional role of biota?

- **Responses and feedbacks to biological, climatic and geological perturbations and global change. The Earth's surface dynamic system**: How can we use observatories to predict the

future of the critical zone? How do processes with small characteristic time and limited spatial imprint influence the longer time-scales and larger spatial scales? Can we predict critical zone trajectories?

In order to answer to those questions, the French project CRITEX has been funded to acquire or develop adequate equipments to perform a state-of-the-art temporal and spatial exploration of the critical zone. The different work-packages of CRITEX focus on two main challenges: to be able to perform high frequency measurements and to study in detail hot-spots and hot-moments (Fig. 1.3).

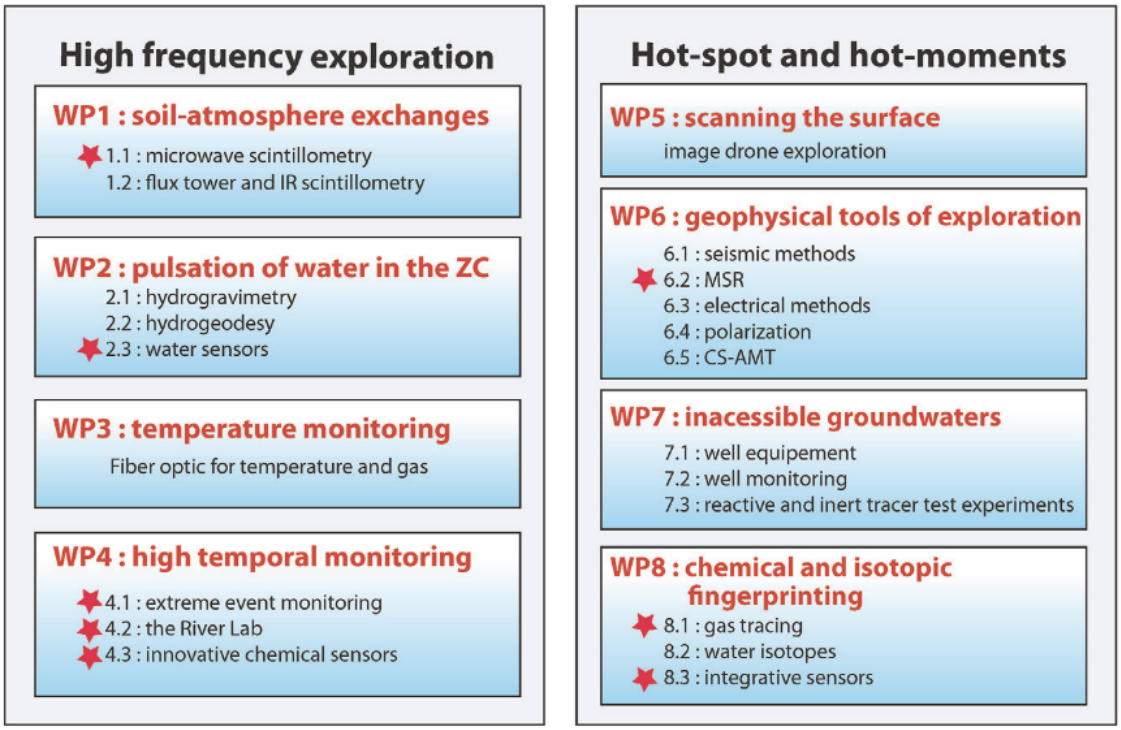

Figure 1.3: Distribution of the CRITEX work packages (Gaillardet et al., 2018).

Using geophysical tools to study the critical zone One can see that geophysical tools are well represented in the work-packages of the CRITEX project and it is the kind of tools that I decided to work on and develop. Indeed, if geophysical methods have been previously developed for mining and oil & gas reservoir applications, their sensitivity to parameters and processes of interest make them essential to study the critical zone. During the last two decade a new discipline is emerging: the hydrogeophysics. The American Geophysical Union (AGU) Hydrogeophysics Technical Committee, upon which I am a member since 2015, proposes the following definition:

> "***Hydrogeophysics*** *involves use of geophysical measurements for estimating parameters and monitoring processes that are important to hydrological studies, such as those associated with water resources, contaminant transport, ecological and climate investigations. Improved characterization and monitoring using hydrogeophysical techniques can lead to improved management of our natural resources, understanding of natural systems, and remediation of contaminants.*" (`http://hydrogeophysics.org/`)

Hydrogeophysics as a discipline has been the subject of many books (e.g., Rubin and Hubbard, 2005; Vereecken et al., 2006), book chapters (e.g., Hubbard and Linde, 2011), and review papers (e.g., Binley et al., 2015; Parsekian et al., 2015) over the years. This discipline starts to be pretty established in the critical zone research community, and there is a real need for the formation of a new generation of scientists to correctly use and push further the development of these tools. This

yields to initiatives such as the organization of workshops, summer schools (i.e., Cargèse Summer School: https://cargese2018.sciencesconf.org/), and Innovative Training Network (ITN) at the European scale (i.e., the ENIGMA ITN), that are oriented towards hydrogeophysics.

Among other initiatives, the ENIGMA ITN, for European training Network for In situ imaGing of dynaMic processes in heterogeneous subsurfAce environments, is funded by the Marie Sklodowska-Curie action grant of the European Union's Framework Programme for Research and Innovation H2020 (https://enigma-itn.eu/). Its goal is to train a new generation of 15 young researchers in the development of innovative methods for imaging process dynamics in subsurface hydrosystems, in order to enhance understanding and predictive modelling capacities and to transfer these innovations to the economic sector (Fig. 1.4). The 15 young future PhD students will contribute to develop the spatial representation of subsurface heterogeneity, fluxes, chemical reactions and microbial activity, through the integration of data and approaches from geophysics, hydrology, soil physics, and biochemistry. The network ENIGMA gather 21 partners (15 academic and 6 industrial) from 8 European countries. The Enigma ITN started in January 2017 and will run until December 2020, I serve as deputy coordinator of the project.

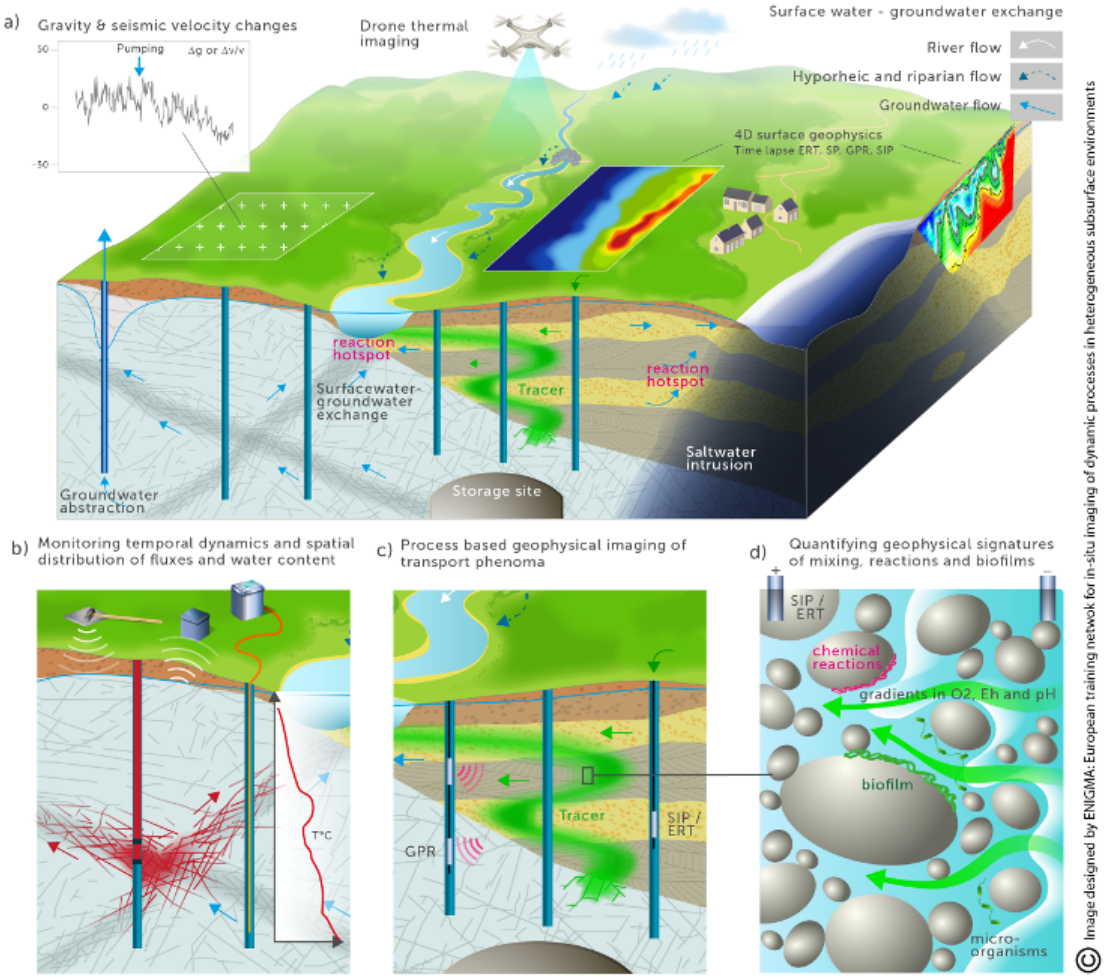

Figure 1.4: Overview of geophysical methods used and developed in the ENIGMA ITN (enigma-itn.eu): (a) general view, (b) from surface to boreholes, (c) cross holes, and (d) at the small scale (Credits: ENIGMA ITN).

As hydrogeophysics attracts an increasing number of users in the research community due to its interest to study the critical zone, many limitations start to be unveiled, generating motivation for new researches, inducing theoretical and technical developments. First, the geophysical instrumentation has been drastically improved over the last two decades, providing user friendly tools with faster

acquisition (i.e., multi-channel acquisition) and better accuracy. Then, inversion algorithms and increasing computing power is allowing paradigm changes in imaging strategies (i.e., joint inversion approaches) and uncertainty characterization (i.e., from deterministic to stochastic inversion). Finally, more theoretical investigation, such as physical and mathematical developments or laboratory works, are continuously improving our understanding of how the measured geophysical signal is generated by state properties or processes of interest in critical zone studies: namely the petrophysical relationships.

In the present document, I propose a synthesis of the works I have been conducting since my PhD defence in 2009 to improve the way we use hydrogeophysics. Most of it falls under that third topic, that is developing and testing new or better petrophysical relationships. In a nutshell, my work of the last decade could be summarized by the following question: **how to better take into account heterogeneities in the geological media at the mesoscopic scale in the generation of geophysical signals for hydrology and critical zone studies ?**

The first chapter will present some theoretical bases such as: the principles of the different geophysical methods I have been using and developing and the definition of what does mesocopic scale refer to in hydrogeophysics. In the second chapter, I will present the work related to mesoscopic heterogeneities under partial saturation and its impact on water flow and transport properties. In the third chapter, I will present my work related to fractures and fracture network and how they affect geophysical signatures. The fifth chapter then deals with a field that I am just starting to explore, the influence local heterogeneities related to biogeochemical reactions. The last chapter is dedicated to some conclusion on these works and outlook for future ones.

Chapter 2

Methods and definitions

Geophysics covers a large range of research areas using a large variety of tools (relying on different physical principles) at various scales (from the pore to the entire earth). Geophysical measurements can be made from the surface or within a geological medium, but also on samples in laboratory conditions. They are generally considered to be not (or less) intrusive and less expensive than most other techniques (i.e., drilling, excavation). They also present the big advantage to be repeatable (e.g., time-lapse) and therefore allow the monitoring of state changes of the geological target.

The present chapter is restricted to only a couple methods that can be used to study the critical zone: the one I used and/or developed while conducting my research during the last decade. This short presentation is therefore not exhaustive.

2.1 Presentation of the considered geophysical methods

2.1.1 Electrical resistivity and induced polarization

Electrical resistivity and induced polarization represent a familiy of active geoelectrical technics that have been discovered by the Schlumberger brothers a century ago: in 1912 for the Direct Current (DC) resistivity (Schlumberger, 1912) and in 1920 for the Induced Polarization (IP) effect (Schlumberger, 1920). As presented in detail by Binley and Kemna (2005), one can identify three different methods:

- DC resistivity
- Time Domain Induced Polarization (TDIP)
- Frequency Domain or Spectral Induced Polarization (SIP)

Electrical resistivity The measurement of the DC resistivity relies on Ohm's law, it consists in injecting an electrical current in a geological medium and measure the resulting electrical potential differences to determine its electrical resistivity (or its reciprocal, the electrical conductivity). The electrical conductivity of a medium is strongly affected by key properties such as (for a review, see Glover, 2015): texture and structure (e.g., porosity, pore connectivity, fracturation), the lithology (e.g., the clay content), fluid saturation (e.g., water saturation), the pore water chemical compositions (e.g., salinity). During my PhD thesis, I worked on petrophysical relationships to relate the electrical conductivity with different transport properties such as the ionic diffusion coefficient (Jougnot et al., 2009), the thermal conductivity (Jougnot and Revil, 2010), or the hydraulic conductivity in partially saturated conditions (Jougnot et al., 2010b).

Induced polarization Induced polarization measurements can be divided in two approaches: time domain and frequency domain measurements. In IP measurements, dielectric phenomena (i.e. polarization) are also taken into account. It is part of the low frequency electro-magnetic methods. Therefore, the property of interest is not only the resistivity, but rather the complex resistivity (or impedance).

Figure 2.1 illustrates the principle of TDIP measurements. Similarly to DC resistivity, a current is injected in a medium to obtain its electrical resistivity. But, when the current injection is stopped, the relaxation of the electrical potential differences is also measured. Monitoring this decrease is a way to determine how fast the medium de-polarize, that is to obtain its chargeability.

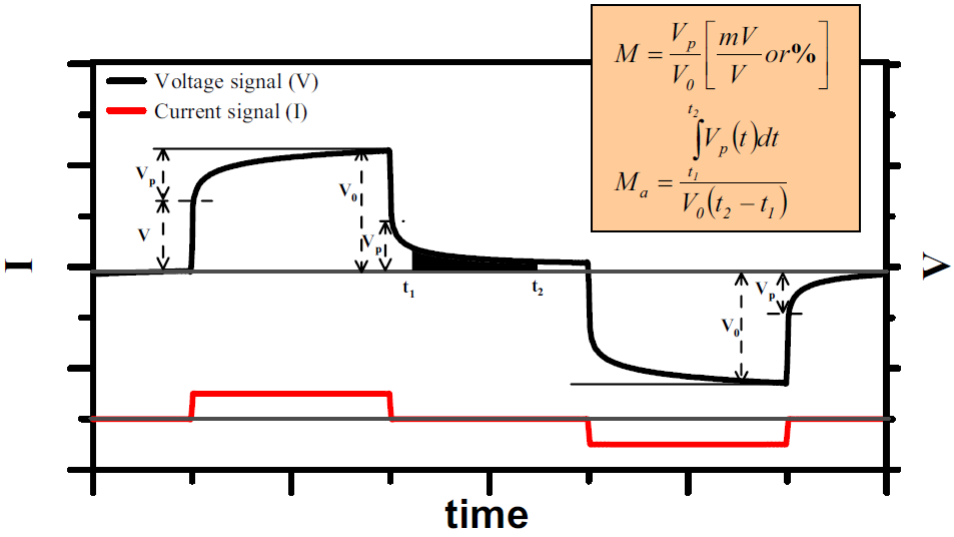

Figure 2.1: Principle of the Time Domain Induced Polarization method (from Ghorbani, 2007).

Figure 2.2 presents the principle of SIP measurements. In this case, the current is injected using a sinusoidal function with a given frequency (Fig. 2.2a) and the resulting voltage is measured. This resulting voltage also has a sinusoidal shape with a different amplitude and a phase lag. The electrical resistivity is obtain from the amplitude and Ohm's law, while the phase, usually negative, is related to the chargeability of the medium. By sweeping this measurements over a large range of frequencies, typically from 1 mHz to 10 kHz, one can obtain the amplitude (i.e., resistivity) and phase (i.e., related to the chargeability) spectra of the complex resistivity (Fig. 2.2b).

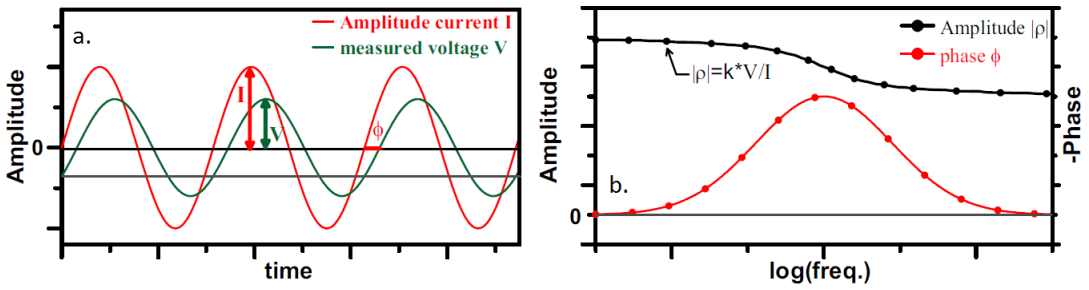

Figure 2.2: Principle of the Spectral Induced Polarization method (from Ghorbani, 2007).

Like the resistivity, the chargeability (or the phase) of a geological medium can be related to many parameters of interest such as: the clay content (through the cationic exchange capacity), the fluid phase composition (e.g., water saturation, presence of pollutant, chemical composition). During my PhD thesis I did study the effect of the clay rock dessication on several parameters obtained by SIP (Ghorbani et al., 2009; Jougnot et al., 2010b) and proposed a mechanistical model to explain

part of the polarization phenomena (Jougnot et al., 2010a). Many works on TDIP or SIP try to relate the chargeability or phase information to predict the permeability of porous media (e.g., Revil and Florsch, 2010; Zisser et al., 2010).

These DC resistivity and IP measurements can be on sample using a fixed measurement set-up or they can be displaced to image geological media. This imaging technique is called Electrical Resistivity Tomography (ERT) for DC measurements and Electrical Impedance Tomography (EIT) for IP measurements. The principle of electrical tomography from the surface is illustrated by Fig. 2.3. Displacing current and potential electrodes allow us to scan the subsurface and obtain apparent properties (i.e., apparent resistivity). Then, inversion algorithms can be applied to retrieve the "true" property distribution (resistivity and chargeability or phase) (e.g., Binley and Kemna, 2005).

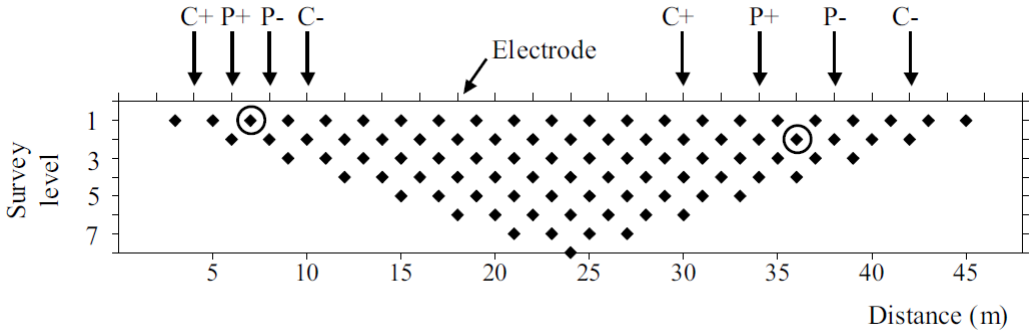

Figure 2.3: Principle of geoelectrical imaging (from Binley and Kemna, 2005).

2.1.2 Self-potential

The **Self-Potential** (SP) is a passive geophysical method that consists in measuring the naturally occurring electrical field at the surface or within a geological medium. It is one of the oldest geophysical methods (see Fox, 1830).

The measurement principle of SP is rather simple one, as illustrated in Fig. 2.4, SP measurements can be done with only two non-polarizable electrode (e.g., Petiau, 2000) and a high impedance voltmeter. One can measure and represent it as SP profiles, 2D maps, 3D electrical field, or time series. However, as pointed by Susan Hubbard in the foreword of Revil and Jardani (2013)'s book on the SP method:

> "*Although self-potential data are easy to acquire and often provide good qualitative information about subsurface flows and other processes, a quantitative interpretation is often complicated by the myriad of mechanisms that contribute to the signal.*" S. Hubbard

The different sources generating SP signal can be divided in two kinds:

- Electro-kinetic: related to water flow (streaming potential)
- Electro-chemical: related to concentration gradient (diffusion or junction potential), thermal gradient(temperature potential), or redox gradients (redox potential)

These sources are additive and often superposed when measuring the electrical field. Their relative contributions to the total SP signal depends on the medium conditions and processes (e.g., Jouniaux et al., 2009; Revil and Jardani, 2013).

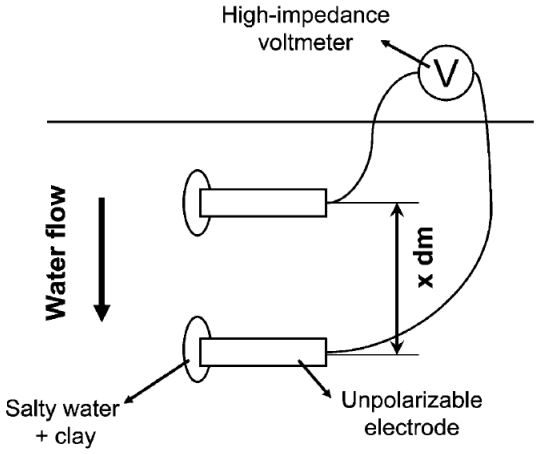

Figure 2.4: Principle of the Self-Potential measurement (from Darnet and Marquis, 2004).

Electrokinetic contribution SP signals of electrokinetic nature have been studied since Quincke (1859) and quantified by modeling since Helmholtz (1879) and von Smoluchowski (1903). They are link to the presence of an Electrical Double Layer (EDL) at the interface between the mineral and the pore water, that is the presence of an excess of charge in the pore solution that counterbalance free charges at the mineral's surface. When the water flows into the pores, it drags this excess charge, generating an charge separation and thus the so-called streaming current. These signals are usually referred to as ***Streaming Potential***. During my PhD thesis, I started to work the mechanisms of these phenomena under partially saturated conditions (Linde et al., 2007; Revil et al., 2007).

Electro-diffusive contribution The presence of ionic concentration gradient in solutions yields to the diffusion of the ions towards smaller concentrations. When the ions do not have the same mobility an electrical current is generated to make them diffuse at the same velocity in order to respect the local electro-neutrality of the system. This phenomenon is also known as junction potential. In addition to this effect, the presence of electrical double layers, i.e, zones from where anions are partially or totally excluded can enhance of diminish this current generation. I worked on these phenomena in clay rocks during my PhD thesis (Revil and Jougnot, 2008; Jougnot et al., 2009).

Thermo-electric contribution When submitted to thermal gradient, ions also tend to diffuse as their mobility strongly depends on the temperature. This phenomenon is described in details by Leinov and Jackson (2014).

Redox contribution This corresponds to the first application of the SP method, i.e., localizing ore bodies for the mining industry Fox (1830). When an electronic conductor (e.g., ore body, metallic pipe, bacterial nano-wires) connects two domains with different redox potential, it acts as a "***geo-battery***", generating electrical current and electrical potential differences that can be significantly larger than the other contributions. It is important to note that if no electronic conductor connect the regions with different redox potentials, the electrical circuit is open and thus no electrical current nor electrical potential difference is generated.

The SP signal measured in natural media are therefore a superposition of potentially all these contributions. It is worth noting that the electrical resistivity of the geological medium has a strong influence on the amplitude of the SP signals. Hence it is crucial to determine the electrical resistivity of the medium in order to quantitatively approach the SP signal.

2.1.3 Seismic and seismoelectric methods

Over the course of my PhD thesis I mainly worked with the geo-electrical methods presented in the previous sections (i.e., SIP and SP), but during my post-doc at the University of Lausanne, I started to look into completely different, but yet complementary, methods based on wave propagation: seismic and seismo-electric methods.

Seismic methods Seismics methods are active geophysical methods based on the mechanical wave propagation in the subsurface. A seismic acquisition set-up usually consist in a collection of geophones implanted along linear profiles or arrays, at the surface of the ground. The signal come from a seismic source generated by a portable mechanical source (often a hammer for near-surface applications). Depending on the dimensions of the set-ups, the density of the arrays and the energy of the sources, the recorded wavefields can be analysed to image contrasts in mechanical properties of the near-surface (depths from 1 to 100 m, with resolution from 0.1 to 10 m-scale) using the standard equipments available for environmental applications. The most popular interpretation method is refraction tomography (Fig. 2.5) which consists in picking first arrivals times of the wavefield and then to invert for pressure (P) or shear (S) waves velocity models (VP or VS, depending on the type of sources and sensors). As an alternative to S-wave refraction tomography, the recorded wavefield can also be processed to extract surface-wave dispersion data that are then inverted for VS models (e.g., Pasquet and Bodet, 2017).

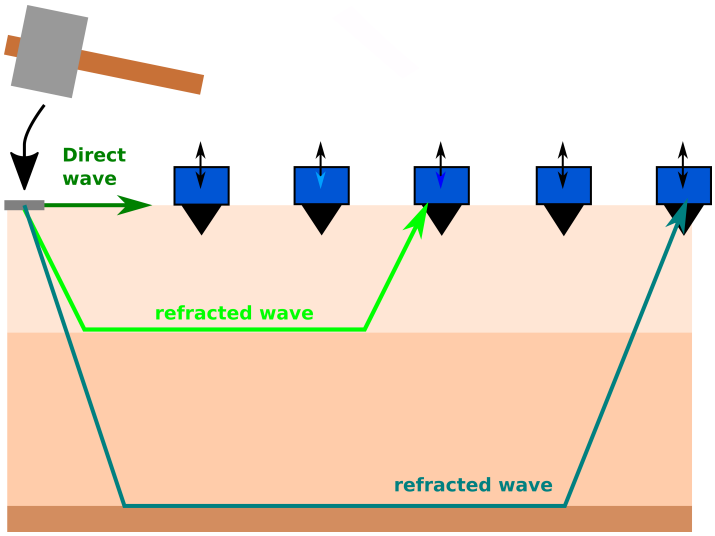

Figure 2.5: Principle of seismic refraction acquisition (Credits: M. Dangeard).

Seismic methods are becoming a common geophysical tool to study the Critical Zone. It was first applied to characterize the underground structures but now tends be more and more used to capture processes such as weathering (e.g., Clair et al., 2015), water content (e.g., Pasquet et al., 2016), or water redistribution (e.g., Dangeard et al., 2018). Indeed, P- and S-wave velocity can be related to the mechanical properties (i.e., density, porosity, fluid content) but also to textural and structural properties (e.g., lithology variation, presence of fractures). VP and VS show are not affect in the same way by saturating fluids, therefore VP/VS or Poisson's ratio are usually estimated to identify them in porous media. However, the attenuation of the signal also carries interesting information regarding similar and complementary properties such as water content (Rubino and Holliger, 2012), medium permeability (Rubino et al., 2012), or fracture connectedness Rubino et al. (2013).

Seismoelectrical method The seismoelectric (SE) method relies on the measurement of an electrical field generated by a seismic source through seismoelectrical conversion. The first observation

of these signals dates back from Thompson (1936) and has been followed by many researches to propose theoretical frameworks explaining these signals during the last century (e.g., Frenkel, 1944; Pride, 1994; Pride and Garambois, 2005; Revil et al., 2015; Jouniaux and Zyserman, 2016).

The seismoelectrical conversion originates from electrokinetic coupling such as for SP signal generation, that is a charge separation due to a moving fluid along a charged surface: e.g., solid-solution (e.g., Leroy and Revil, 2004), air-solution (e.g., Leroy et al., 2012). One can identify three kinds of seismoelectric signal (Fig. 2.6):

- *The co-seismic signal*: as the wave travels through the medium, it induces a relative displacement of the pore water along mineral surfaces, therefore a charge separation. This is the first identified SE signal in Thompson (1936). This signal travels with the wave and can only be detected as the wave reaches the array of measuring electrodes.

- *The interface response*: as the wave crosses some discontinuity in the medium, that is a contrast in porosity, permeability, water content or any other property affecting the wave velocity, medium electrical conductivity, or excess charge density (see Mahardika et al., 2012, for a didactic example). This signal travels faster than seismic wave (i.e., electromagnetic wave) and is used to detect medium interface (e.g., lithology contrasts).

- *The mesoscopic signal*: this kind of signal is related to compressibility contrast at the mesoscopic scale along the wave path, it will be described in details in the chapter 4 (e.g., Jougnot et al., 2013).

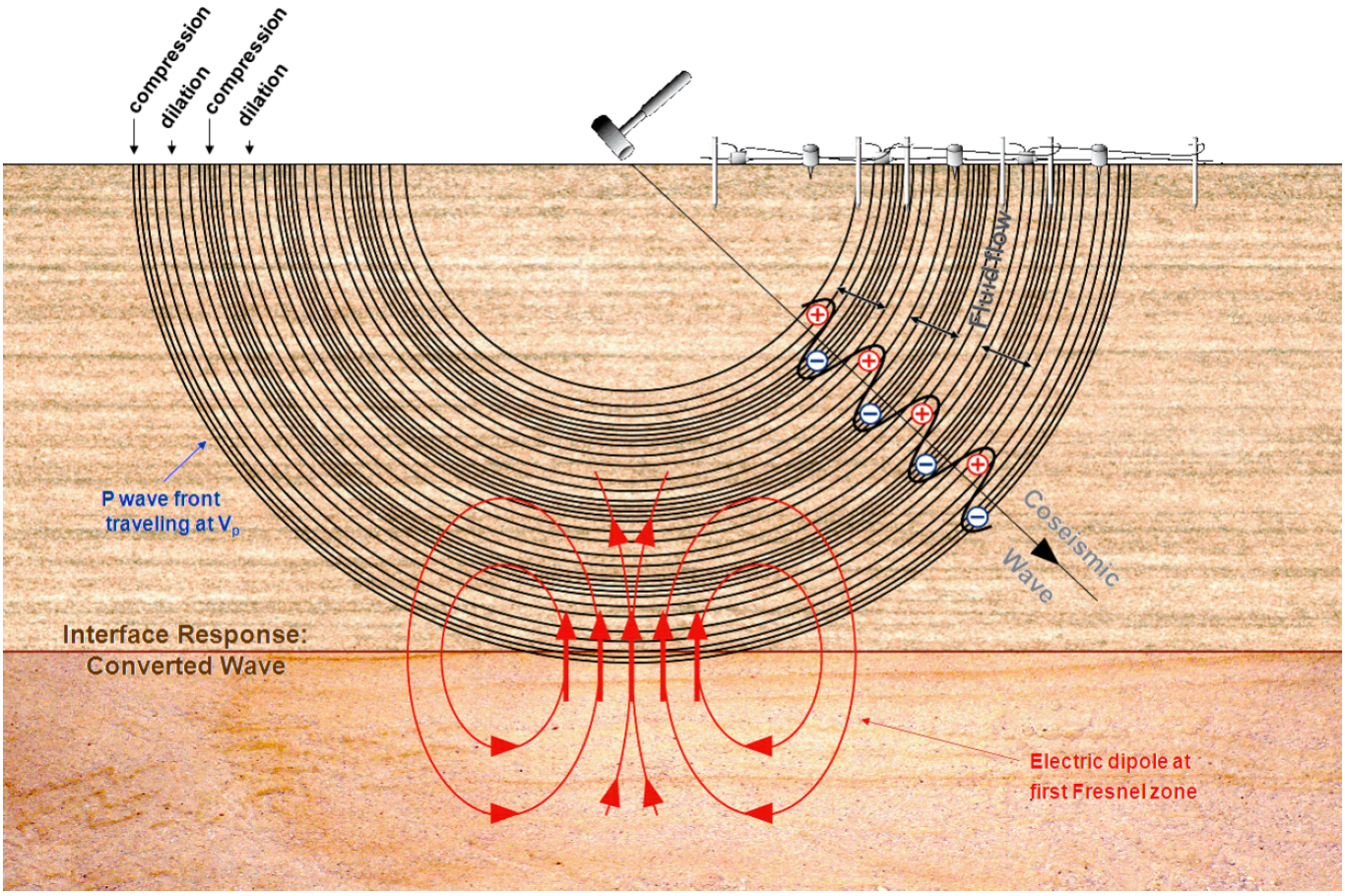

Figure 2.6: Principle of the Seismo-Electrical measurements (from Holzhauer and Yaramanci, 2011).

2.2 Definition of the mesoscopic scale

2.2.1 Scales in critical zone studies

Scales are of tremendous importance in geosciences given the fractal nature of the world we live in (Maldelbrot, 1983). But when dealing with critical zone studies, this question of scales becomes even more crucial as features at the smallest scales can influence properties at the largest one (Fig. 2.7).

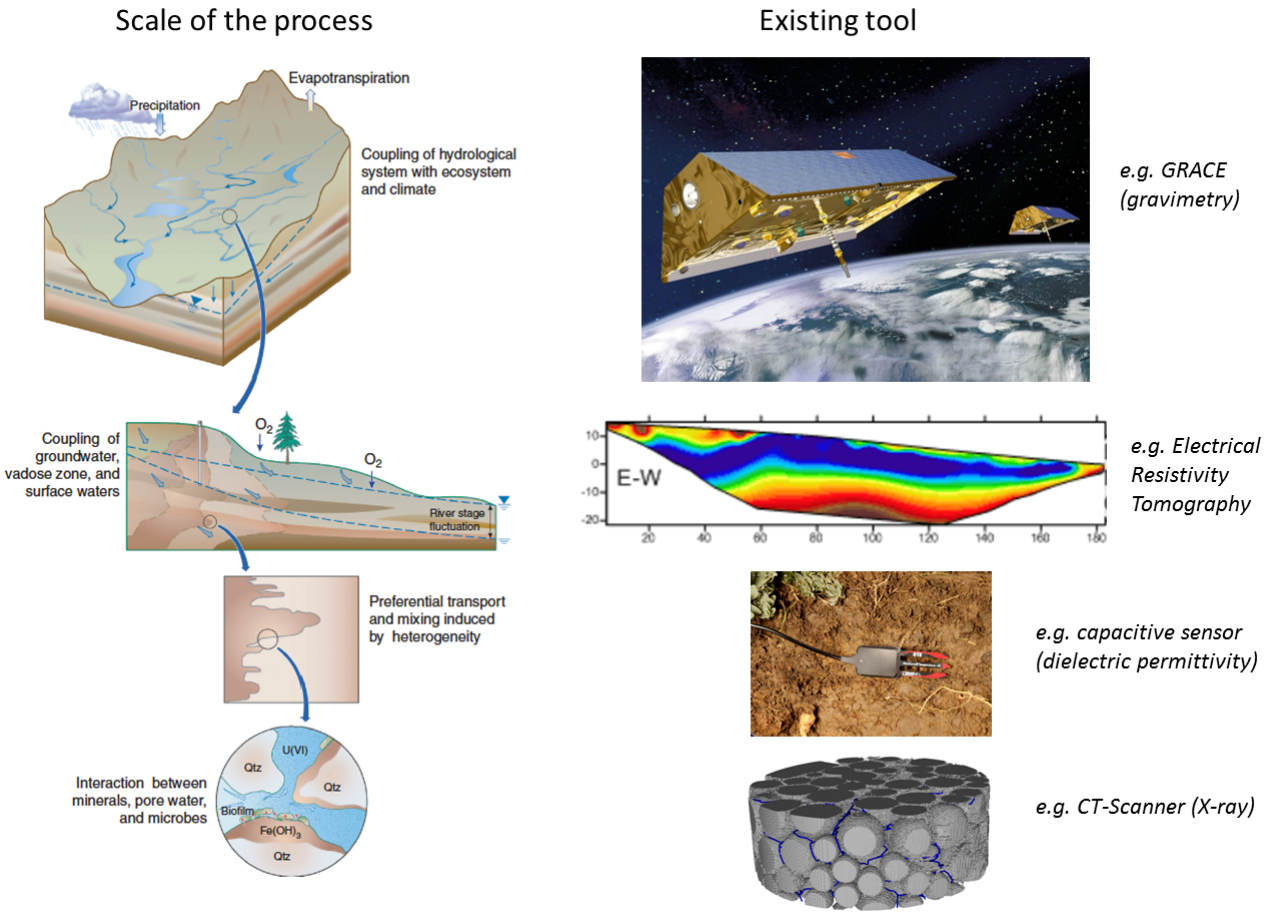

Figure 2.7: The importance of scales in critical zone studies (modified from Hubbard and Linde, 2011).

For example, mineral surface roughness and evolving pore space geometry (e.g., dissolution) affect water flow at the pore scale. The heterogeneity of these properties in turns results in preferential flows that can drive non-darcean or anomalous solute transport at larger scale making it difficult to model or predict contaminant transport at the human scale (drinking wells). Then, it can also drive flow pattern at catchment scales, generating a distribution of water saturation or erosion rate that can shape landscapes (geomorpholgy) or vegetation distribution (ecohydrology). Such analysis could be perform with any kind of heterogeneity or process of various disciplines such as physics, chemistry or biology.

Hydrogeophysical methods have a great interest for studying the critical zone as it provide physical tools at all existing scales. It goes from X-Ray imaging at the micrometer scale to perform tomography of laboratory samples to gravity field measurements at kilometers scale for water distribution monitoring on the earth (i.e. GRACE). In between these two extreme scales, a lot of hydrogeophysical methods exist such as the one presented in section 2.1.

My work as mainly been focused on scales comprised between the nanometer (e.g., distribution of ions in the electrical double layer in Jougnot et al., 2009) to the kilometer (e.g., long ERT profile in

Gélis et al., 2010). The methods presented in section 2.1 have the great interest to be able to be used on geological media across circa 5 orders of magnitude of length scales (from 10^{-2} to 10^{3} m), but they suffer from limited resolution (e.g., Day-Lewis et al., 2005) that can't be better than the sensors spacing or the wavelength (in the best case scenario).

2.2.2 Identifying the mesoscopic scale

Since my first research project during my master "*Experimental and numerical study of hydraulic conductivity in partially saturated double porosity soils*" (Jougnot et al., 2008), I mainly worked on heterogeneous media. Measurement responses always results from an integration over a certain volume. I will detail in the following chapters all the kind of heterogeneities I'm referring to (multiple porosities, cracks, fracture, partial saturation, chemical or energy gradients), but from all those works I could extract a common property: all my measurements where done at a resolution scale which was larger than the scale of the heterogeneity I was looking at. But it is only during my post doc that I came across the concept and a clear definition of the mesoscale.

The mesoscopic scale Müller et al. (2010) proposes a clear and simple definition of mesoscale or mesoscopic scale for seismic properties: it is the scale which is comprised between the pore scale and the measurement scale (Fig. 2.8). In seismic (and seismoelectric) methods the measurement scales depends on the wave length, but this concept can be used in all the other geophysical methods. Considering the electrical methods presented above (DC, TDIP, SIP, and SP), the measurement scale roughly correspond to electrodes spacing and its resolution decreases with the distance from those. In addition to the physical limitation of the measurements, one also has to account for resolution loss during the inversion/reconstruction process.

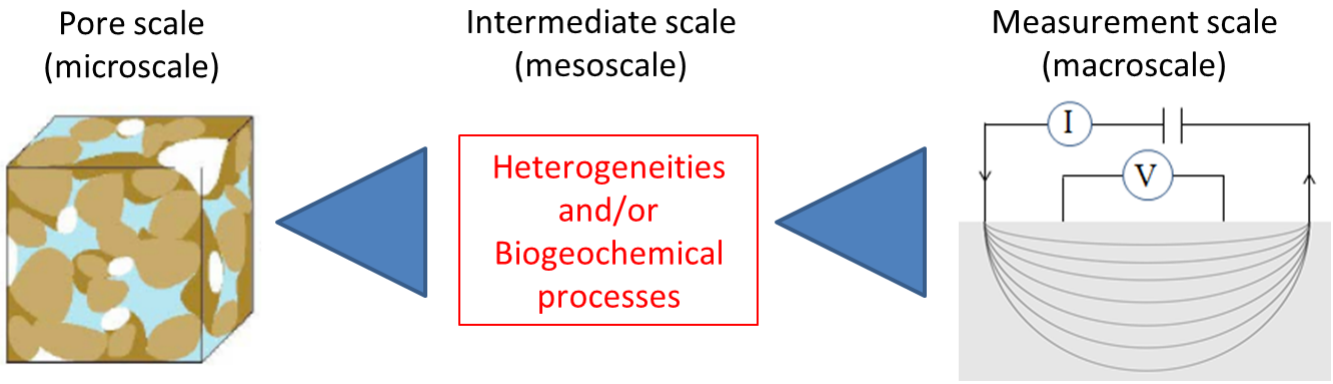

Figure 2.8: Identification of the mesoscale.

In hydrogeophysics, the measurement scale does not always correspond to a Representative Elementary Volume (REV). Indeed, many contrasts in the structures, properties or processes existing at the mesoscopic scale affect the measurements in a way that cannot be easily described by an effective property. Nevertheless, a single geophysical measurement can only produce a given datum. The challenge when dealing with mesoscopic heterogeneities is to link the measured signal to the heterogeneity or process that generates it.

The mesoscopic heterogeneities During the last decade, I have been studying different kind of meso-scale heterogeneities and processes that I regroup here in three thematic chapters:

- **Water distribution in saturated and partially saturated porous media**: porous media usually exhibit a certain heterogeneity in term of pore size distributions (PSD). From this mesoscopic heterogeneity result spatially distributed properties (e.g., porosity, permeability, water content) that can strongly affect flow and transport (e.g., preferential flow, non-darcean transport).

- **Fractures and fracture networks in porous media**: single fractures and interconnected fracture networks are probably one of the most contrasted kind of heterogeneities as it create strong local gradient in properties between the fracture and the matrix, also controlling flow and transport.

- **Heterogeneities generated by transport and biogeochemical reactions**: the critical zone is characterized by a large ranges of coupled processes of different nature (e.g., geochemical, biological). This reactivity also occurs with a certain spatial distribution in the medium: water and solute transport transport can either stop or reinforce these biogeochemical reactions by modifying local chemical and biological states (e.g., ionic concentrations, redox potentials, biochemical equilibrium).

Chapter 3

Water distribution in saturated and partially saturated porous media

Partially saturated media are intrinsically heterogeneous as some pores are saturated by water while others are by gas (e.g., air) or by a non aqueous liquid phase (e.g., oil, organic contaminant). The spatial distribution of the water in porous media largely depends on the pore size distribution (PSD) (e.g., Bear, 1988) but can also depend on what happened to the medium (see Soldi et al., 2017, for an example about hysteretic effects). The porous medium structure and PSD can affect the water flow and transport distributions at the mesoscopic scale in both saturated and partially saturated conditions, but it is even more important under partially saturated conditions.

In this chapter, I present some of my works related to the effect of these heterogeneities on two main geophysical methods: electrical conductivity (section 3.1) and the self-potential (sections 3.2 and 3.3).

3.1 Effect of preferential flow and transport on electrical conductivity

3.1.1 Development of a millifluidic geophysical set-up

One of the main problems with studying rocks is to achieve non-destructive control of on-going processes. If geophysical methods are really powerful tools to monitor these, their integrative nature, the indirect measurements they provide and their limitations in term of resolution cannot allow to directly look into the studied media (see previous chapter).

During the last decades, increasing interest in milli- and micro-fluidic system have yield to technical developments in many research fields, from physical to biological disciplines. de Anna et al. (2013) and Jiménez-Martínez et al. (2015) proposed interesting new millifluidic set-ups to study flow and transport in porous media. They developed a modified Hele-Shaw cell (i.e., two parallel glass plates separated by a very small aperture) by inserting vertical cylinders acting as obstacles for the flow and the transport: a 2D flow cell. Transport in the cell is monitored by a camera sensitive to the concentration of a fluorescent tracer in the pore fluid. The cell is designed to perform studies in two phase flow conditions (e.g., water and air).

In 2013, we adapted their millifluidic set-up by inserting copper electrodes in the flow cell in order to be able to monitor both the ionic concentration distribution at the microscopic scale with the camera (i.e., with several pixels per pore) and at the macroscale with the resistivity meter (i.e., one value for the entire cell). This experiment, presented by Jougnot et al. (2018), is, to the best of my knowledge, the first designed millifluidic geophysical set-up (Fig. 3.1). We used this set-up to monitor the saline tracer test in both saturated and partially saturated conditions.

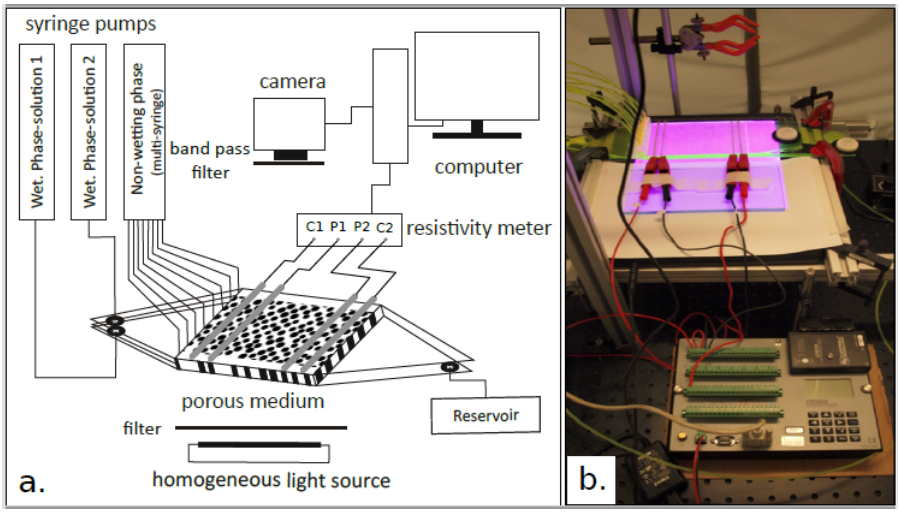

Figure 3.1: (a) Sketch and (b) picture of the millifluidic geoelectrical set-up used in Jougnot et al. (2018). It corresponds to the set-up proposed by Jiménez-Martínez et al. (2015) that we adapted to monitor electrical conductivity in the flow cell during a tracer test experiment.

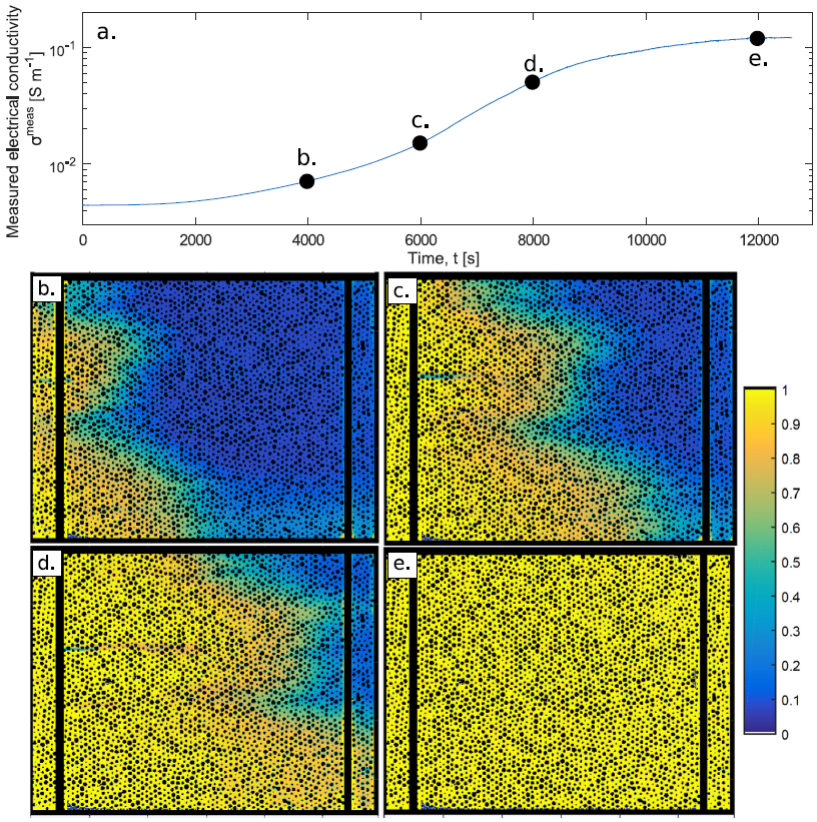

Figure 3.2: (a) Evolution of the electrical resistivity during the tracer test under fully saturated conditions. (b-e) four snapshots of the percolation of the tracer in the flow cell (from Jougnot et al., 2018).

3.1.2 Geolectrical monitoring of a saline tracer test at the mesoscopic scale

Prior to the saline tracer tests, we characterized the petrophysical properties of the flow cell, i.e., determining its formation factor and the saturation index from Archie (1942). This was done by saturating the cell homogeneously with a solution of a known concentration and electrical conductivity, then draining the cell to obtain partially saturated conditions. We repeated this procedure with different salinities to make sure that the surface conductivity of the material was negligible (see Fig. 4 of Jougnot et al., 2018).

We conducted the first tracer experiment under water saturated conditions. Saturating first the column with the background solution, prior to the injection of the saline tracer. Figure 3.2a shows the increase of the bulk electrical conductivity as the tracer percolate fairly homogeneously in the flow cell. As the saline tracer percolate in the medium, its becomes in contact with both potential electrodes (P1 and P2), creating a slow and progressive step increase in the effective electrical conductivity of the medium between t = 4000 s and 8000 s (Fig. 3.2a).

For the second tracer experiment, we established a partially saturated conditions with the background solution prior to the tracer injection. It yields a much more complex geometry for its percolation due to the presence of the air bubbles (in white in Fig. 3.2). As we inject the tracer at a constant flow rate, it percolates faster through the flow cell than under water saturated conditions, yielding a clear preferential flow (and electrical current) path (i.e., solute fingering). This results in a sharper step in the measured effective electrical conductivity (from t = 3000 s and 6000 s). Note that, as more tracer fingers connect the potential electrode, smaller steps are visible (t = 10000 s and t = 12000 s). Such preferential phenomena are well know in the literature on transport in porous media and particularly critical for contaminant transfer and/or mixing predictions (Jiménez-Martínez

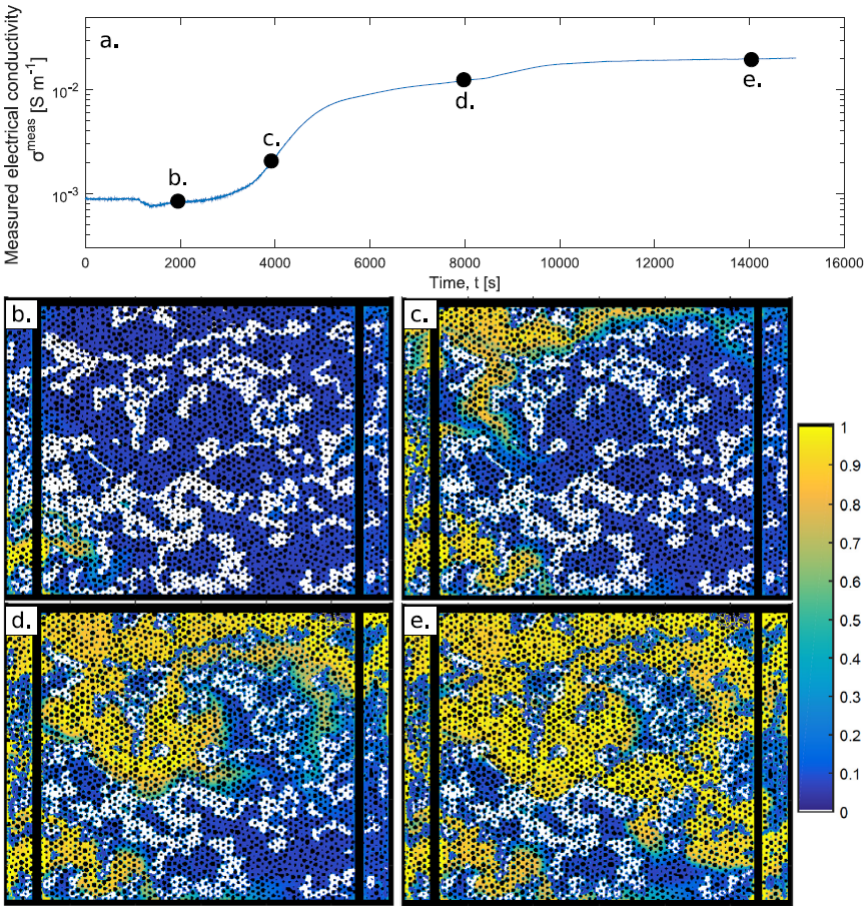

Figure 3.3: (a) Evolution of the electrical resistivity during the tracer test under partially saturated conditions. (b-e) four snapshots of the percolation of the tracer in the flow cell (from Jougnot et al., 2018).

et al., 2015).

3.1.3 Discussion of results from the geoelectrical millifluidic experiments

The experimental results obtained from these experiments, yields to two main finding regarding the effect of the mesoscopic heterogeneities on the effective electrical conductivity at the macro-scale.

Conductive phase "dead-ends" Even in a very well connected porous medium (i.e., perfect 2D connectivity without dead-end pores), the presence of a second phase creates heterogeneities at a scale sightly larger than the pore (i.e., the mesoscale) that affects water flow and solute transport at the cell/measurement scale (i.e., the macroscale). Comparing the measurements under water saturated and partially saturated conditions highlights the influence of these heterogeneities on the effective electrical conductivity. Indeed, these phases dead-ends under partially saturated conditions act as more traditionally studied dead-end pores (e.g., Revil et al., 2018), masking part of the medium to electrical current lines (Fig. 3.4).

Tracer mass loss As a direct result, Jougnot et al. (2018) show that this fraction of the pore space that becomes "invisible" to the electrical current has strong implications for the monitoring of tracer at the larger scale. Indeed, we propose that this phenomenon is responsible for part of the apparent tracer mass loss (up to 90 %) that is often encountered in the literature (Binley et al., 2002; Singha and Gorelick, 2005). If solutions exist to deal with this apparent mass loss at the macroscale (e.g.,

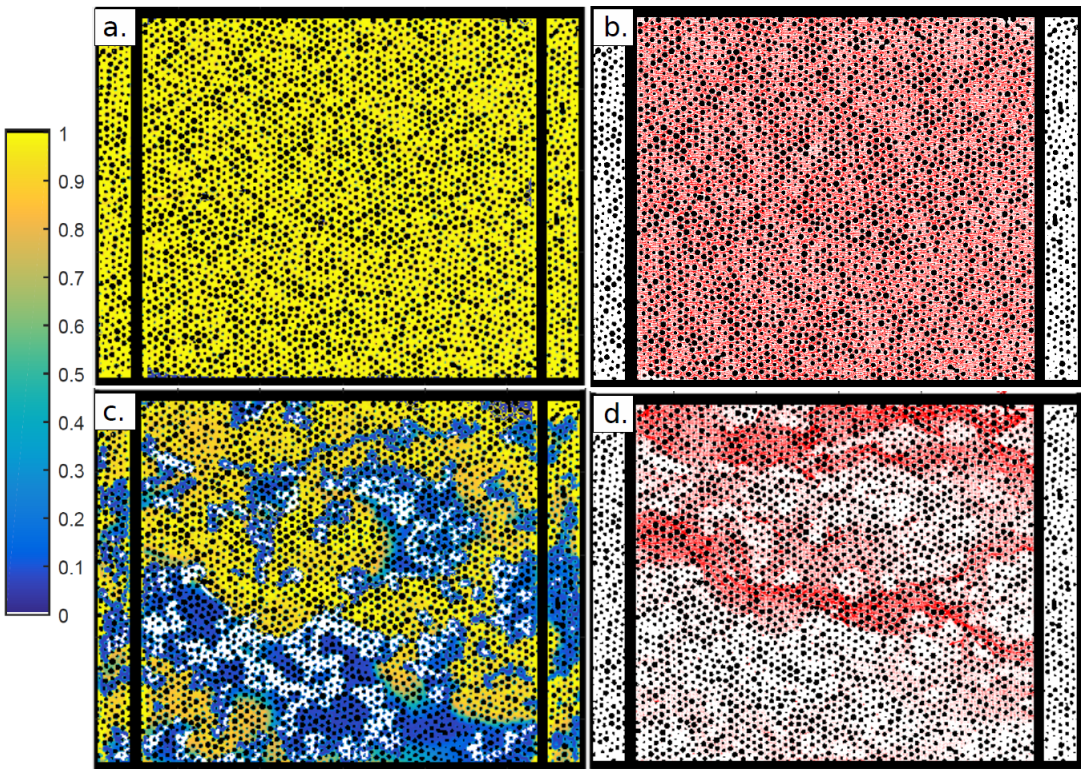

Figure 3.4: (a and c) Normalized tracer concentration and (b and d) current density spatial distribution between the potential electrodes at a late stage of the tracer test experiments under saturated and partially saturated conditions (from Jougnot et al., 2018).

Pollock and Cirpka, 2012; Jardani et al., 2013), we believe that these mesoscale heterogeneities have to be considered using a different approach. Among others, the transposition of dual-domain transport models to geo-electrical petrophysics (e.g., Singha et al., 2007; Briggs et al., 2014; Day-Lewis et al., 2017). Future work with this experimental set-up in collaboration with these authors will likely help us progress to the way to tackle the effects of these mesoscale heterogeneities.

3.2 Streaming current generation in partially saturated porous media

As presented in the previous section, partially saturated media are likely to present heterogeneities due to the distribution of the water in the pore space. Such heterogeneity has to be taken into account when dealing with flow and transport models, but also in the petrophysical relationships that are needed predict the streaming current generation in porous media (see section 2.1.2).

During my PhD thesis, we developed a mechanistic model to predict the effect of the water saturation on the streaming current generation based a volume averaging upscaling method (Linde et al., 2007). This upscaling procedure take into account the volume of each phase (solid, water, and air) to obtain the macroscopic parameters of interest from a microscopic description of the electrokinetic coupling. The fully developed framework can be found in Revil et al. (2007). This approach does not take into account for PSD nor the resulting distribution of water in the porous medium. In this section, I present the results of the works I conducted since my PhD thesis in order to be able to take into account these heterogeneities though a new upscaling procedure that we named the "***flux-averaging approach***".

3.2.1 Flux-averaging approach: numerical upscaling

Figure 3.5 describes the upscaling procedure proposed by Jougnot et al. (2012).

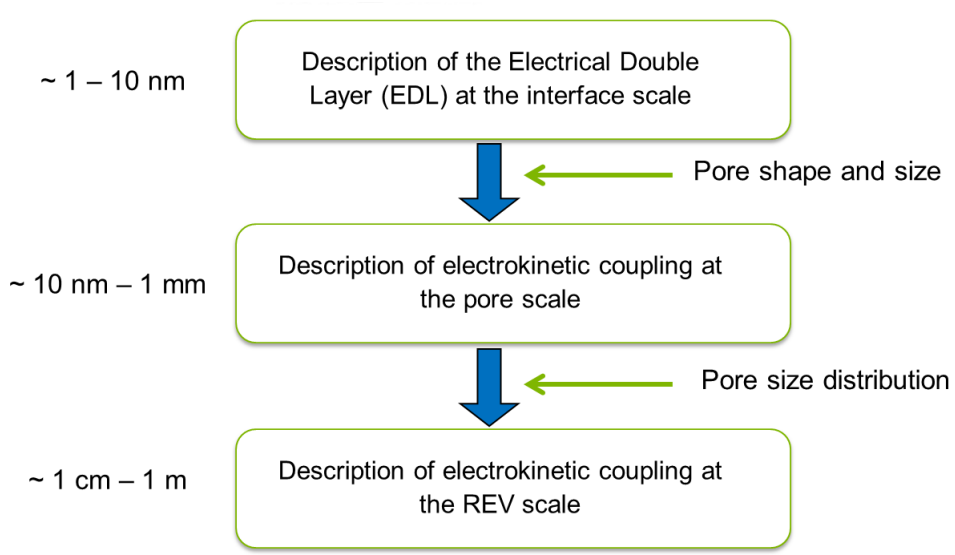

Figure 3.5: Schematic of the flux-averaging upscaling procedure to obtain the effective excess charge density in a porous medium.

Interface scale The first step consists in describing the electrical double layer at the microscale (i.e. a couple of nanometers). As explained in chapter 2, the constituting minerals of a porous medium usually exhibit electrical charges at their surface due to isomorphic substitutions (e.g., Hunter, 1981; Leroy and Revil, 2004). It yields the development of an EDL in the surrounding pore water to maintain the electroneutrality of the entire system (i.e., mineral plus solution). This double layer is an excess of charges (i.e., counter-ions) that counterbalance the mineral surface charges (Fig. 3.6a). A part of these charges are located in the Stern layer, a compact layer that only contains counter-ions (i.e., having the opposite sign compare to mineral surface charges), while the rest of the charges are counter-balanced in the diffuse layer. The diffuse layer contains a net excess of counter-ions but also some co-ions

(i.e., having the same sign as mineral surface charges) due to a weaker influence of the electrostatic surface forces. The distribution of the excess charge in the diffuse layer strictly follows the Poisson-Boltzmann equation, but it can be approximated by a simple exponential function under simplifying assumptions of de Debye-Hückel approximation (see discussion in Jougnot et al., 2019) (Fig. 3.6b).

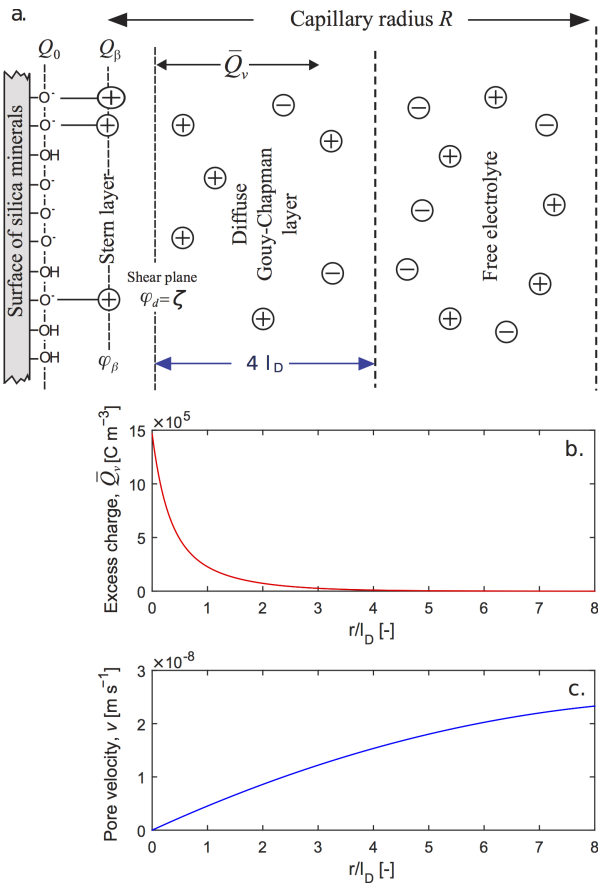

Figure 3.6: (a) Sketch of the EDL at the pore scale. Distribution of (b) the excess charge and (c) pore water velocity in the pore water as function of the distance to the shear plane (from Jougnot et al., 2020).

Pore scale The second step consists in describing the electrokinetic coupling at the pore scale. Based on Jackson (2008, 2010) and Linde (2009), Jougnot et al. (2012) approximate the fraction of the porosity contributing to the water flow as capillaries (stream tubes). This simplified geometry allow an easy determination of the water velocity profile (Fig. 3.6c).

Based on the excess charge and the pore water velocity profile distributions, it becomes possible to determine at what speed which fraction of the excess charge is dragged by the water flow. Averaging the excess charge by the water velocity yields an electrokinetic coupling parameter that we called the ***effective excess charge density*** at the pore scale (see Jougnot et al., 2012).

REV scale As describe in Fig. 3.5, the third and last step is to consider the PSD in a given REV and perform a second flux-averaging upscaling. The effective excess charge density at the REV scale is therefore obtained by weighting the effective excess charge density at each pore by its frequency in PSD function at the REV scale. This parameter is a way to quantify the electrokinetic coupling, and can therefore be used to model the streaming potential generation at the REV scale (for more details, see the book chapter Jougnot et al., 2020).

However, obtaining the PSD of a rock or a soil can be pretty difficult. Among many ways to obtain it, Jougnot et al. (2012) propose to extract the PSD from the hydrodynamic curves (sometimes called

characteristic), that is: from the water retention (WR) or the relative permeability (RP) functions. Those functions describe the evolution of the capillary pressure and the relative permeability with the water saturation, respectively; they directly depend on the medium PSD. They can also be used to obtain which fraction of the pore sizes is saturated by water under partially saturated conditions. Indeed, following the Young Laplace equation (e.g., Bear, 1988), one can relate the capillary pressure of the medium (i.e., its saturation) with the size of the largest capillary that remains saturated (see Fig. 3.7). Therefore, Jougnot et al. (2012) upscaling approach provide a way to determine the effective excess charge density as a function of the water saturation in a porous medium.

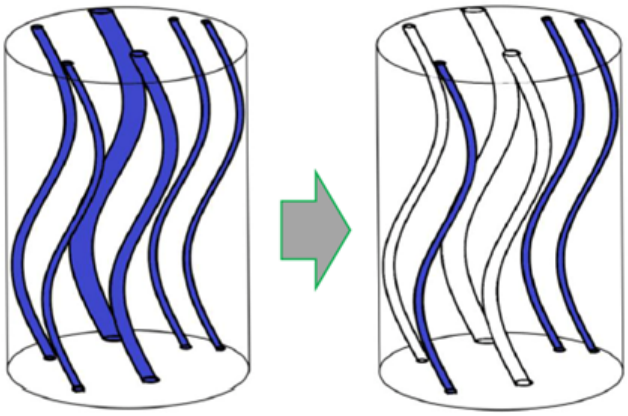

Figure 3.7: Drying of a bundle of capillaries, the larger pores are the first to be drained as the capillary pressure increases.

Figure 3.8a and b present the prediction of the effective excess charge density functions for different typical soil types using the WR and RP approach to extract the PSD using Jougnot et al. (2012), respectively. One can see that the predicted one is highly soil-dependent and predicts an effective excess charge density orders of magnitude bigger than Linde et al. (2007) at low saturations. This is due to the higher density of excess charge in smaller pores (larger influence of surface charge) which remain saturated.

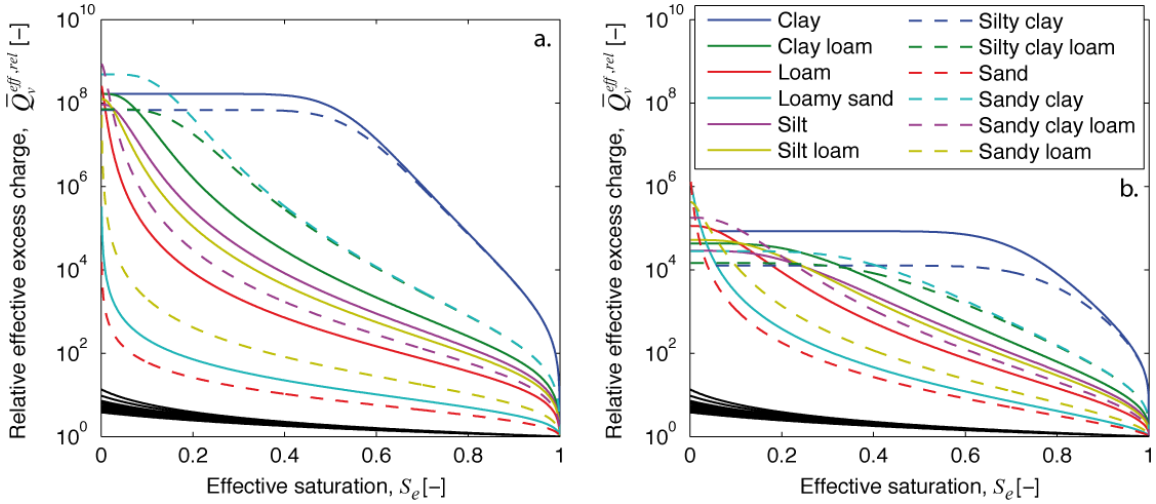

Figure 3.8: Evolution of the effective excess charge density as a function of water saturation for various soil types using the (a) WR and the (b) RP approaches (from Jougnot et al., 2012). The hydrodynamic parameters of the 12 types of soil are the one proposed by Carsel and Parrish (1988).

Note that this numerical upscaling procedure has been sucessfully tested on laboratory and field data. Jougnot and Linde (2013) show that this model correctly predicted the streaming potential

generation in a sand column during drainage and imbibition cycles under well controlled laboratory conditions. The field application will be the subject of a dedicated section further in the text.

3.2.2 Flux-averaging approach: analytical upscaling

One limitation to the numerical upscaling procedure is the computational time needed to determine the effective excess charge density and the availability of the numerical code for others to use.

Development of an closed-form model for water-saturated conditions In Guarracino and Jougnot (2018), we propose an fairly simple analytical solution to determine the effective excess charge density in a closed-form equation for water saturated porous media. This analytical model is based on the same approach than Jougnot et al. (2012) (see Fig. 3.5) with only slight changes and more restrictive assumptions to be able to obtain an analytical solution:

- Assumption 1: The pore water is composed of a binary symmetric 1:1 salt (e.g., NaCl).
- Assumption 2: The pore size must be significantly larger than the diffuse layer thickness (5 times the Debye length).
- Assumption 3: The PSD with which the analytical solution is obtained follows a fractal distribution.

As a results, Guarracino and Jougnot (2018) provide a closed-form equation to predict the effective excess charge depending only on a couple key parameters: to describe the system chemistry and interface properties (ionic concentration, ζ-potential) and petrophysical properties (porosity, permeability, hydraulic tortuosity). Note that the description of the medium PSD does not appear in the closed-form equation.

Figures 3.9 and 3.10 show how well analytical model of Guarracino and Jougnot (2018) perform to predict the effective excess charge density as a function of the ionic concentration and medium permeability, respectively.

Development of an analytical solution under partially saturated conditions Soldi et al. (2019) propose an extension of the model of Guarracino and Jougnot (2018) for partially saturated conditions. Following the concept described in Fig. 3.7, we obtained a closed-form equation taking into account the effect of the water saturation on the effective excess charge density.

Similarly to Guarracino and Jougnot (2018), this new model depends on the chemistry and interface properties (ionic concentration, ζ-potential) and petrophysical properties (porosity, permeability, hydraulic tortuosity), but in addition it also depends on the ratio between the water saturation and the relative permeability. This implies that this closed-form equation is also soil-type dependent (Fig. 3.11). Comparing the model of Soldi et al. (2019) with the previous ones, one can clearly note that it behaves much more like the RP approach from Jougnot et al. (2012) for both amplitude and dependence with saturation.

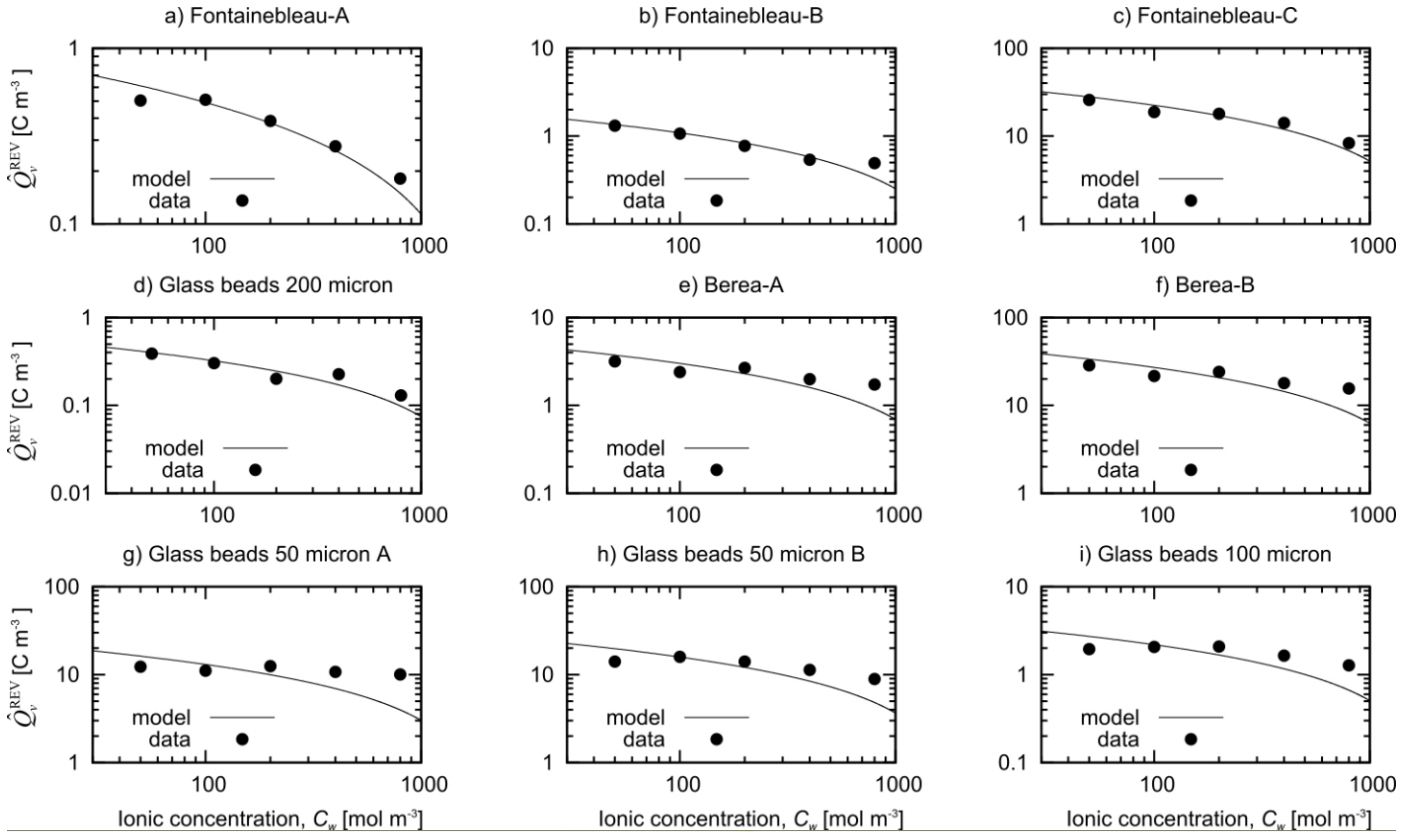

Figure 3.9: Evolution of effective excess charge density with salinity (from Jougnot et al., 2020).

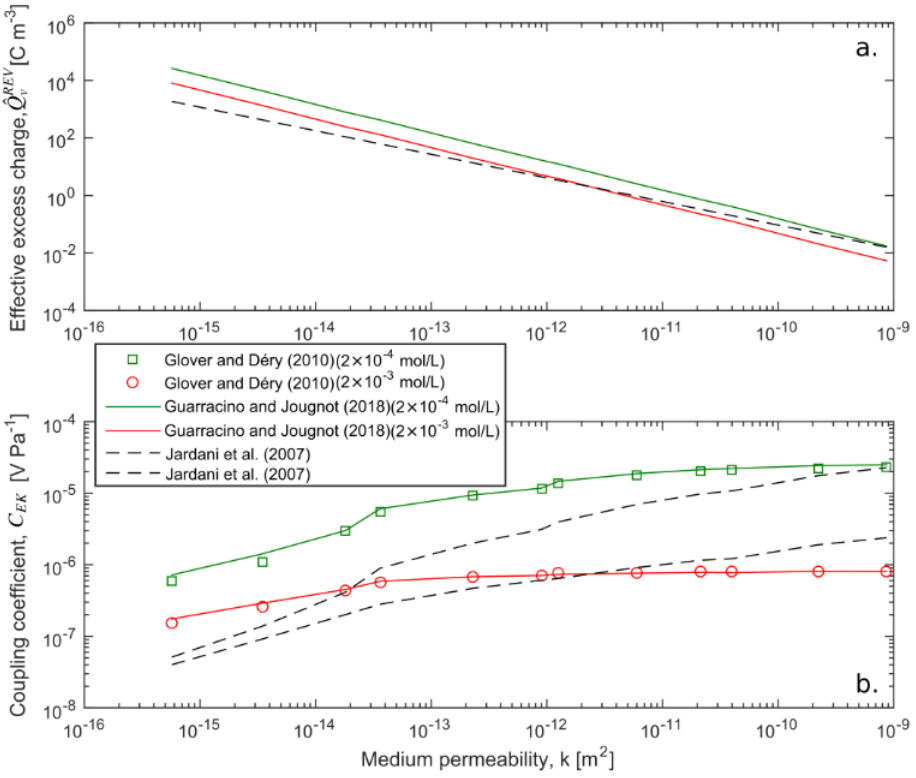

Figure 3.10: Evolution of effective excess charge density with the permeability (from Jougnot et al., 2020).

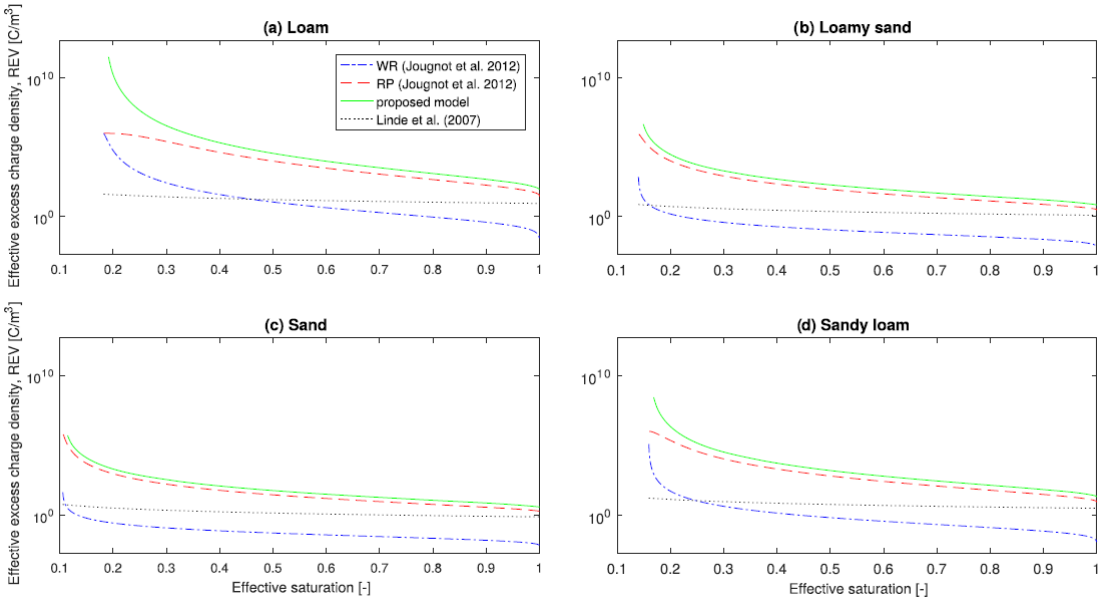

Figure 3.11: Comparison between the models of Linde et al. (2007), Jougnot et al. (2012) (WR and RP appraoches) and the one proposed by Soldi et al. (2019) for four type of soils: (a) loam, (b) loamy sand, (c) sand, and (d) sandy loam (from Soldi et al., 2019).

3.2.3 Study of the effect of the pore size distribution

As discussed in the previous section, the development of the model proposed by Guarracino and Jougnot (2018) is based on a fractal PSD. Even though the closed-form equation does not exhibit an explicit dependence to the PSD, we studied the effect of the PSD on the predicted effective excess charge density.

Jougnot et al. (2019) use a 2D pore network modelling framework (Fig. 3.12a) to predict the effective excess charge density for four different PSD (Fig. 3.12b to e). The simulations were run once for each given distribution (five PSD with different permeabilities for each of the four types) and concentration (nine different concentrations) by solving the electrokinetic system electrokinetic problem at the scale of the entire network. It resulted in 180 pore networks with a size of 100×100 pores, allowing the detailed study of the influence of a large range of permeabilities (from 10^{-16} to 10^{-10} m^2) for different ionic concentrations (from 10^{-4} to 1 mol L^{-1}).

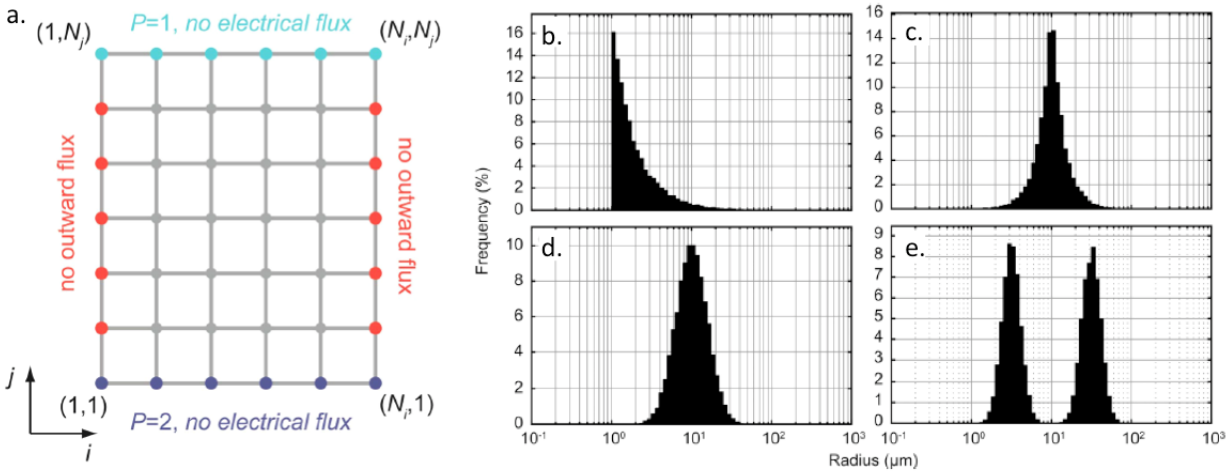

Figure 3.12: (a) 2D Pore network used to compute the effective excess charge density for four types of PSD: (b) fractal, (c) exponential symmetric, (d) lognormal, and (e) double lognormal (modified from Jougnot et al., 2019).

Figure 3.13 presents the results of the pore network simulations (symbols) and the predictions from the model of Guarracino and Jougnot (2018) (lines on Fig. 3.13b). The dependence of the effective excess charge density on both the permeability and the pore water ionic concentration is well taken into account in their model, showing a very good agreement between the simulations and the predictions. The only noticeable discrepancy is for very low permeabilities (smaller pores) and low ionic concentrations (larger Debye lengths), that is when the model assumptions are not fulfilled (see the discussion in Jougnot et al., 2019).

This implies that, in water-saturated conditions, the analytical model based flux-averaging to predict the effective excess charge density takes well into account the meso-scale heterogeneity constituted by the PSD. Further work need to be done to test that under partially saturated conditions.

3.2.4 Opening for seismoelectric models

The prediction of electrokinetic coupling is also of uttermost importance in the field of seismoelectrics (see Section 2.1.3). Bordes et al. (2015) discuss the importance of having a correct description of the electrokinetic coupling coefficient to be able to reproduce the measured co-seismic signal recorded in a laboratory experiment under partially saturated condition.

Recently, Jougnot (2019) extended the flux-averaging approach presented in this sub-section to determine the ***frequency dependent effective excess charge density***. So far, this work is restricted to

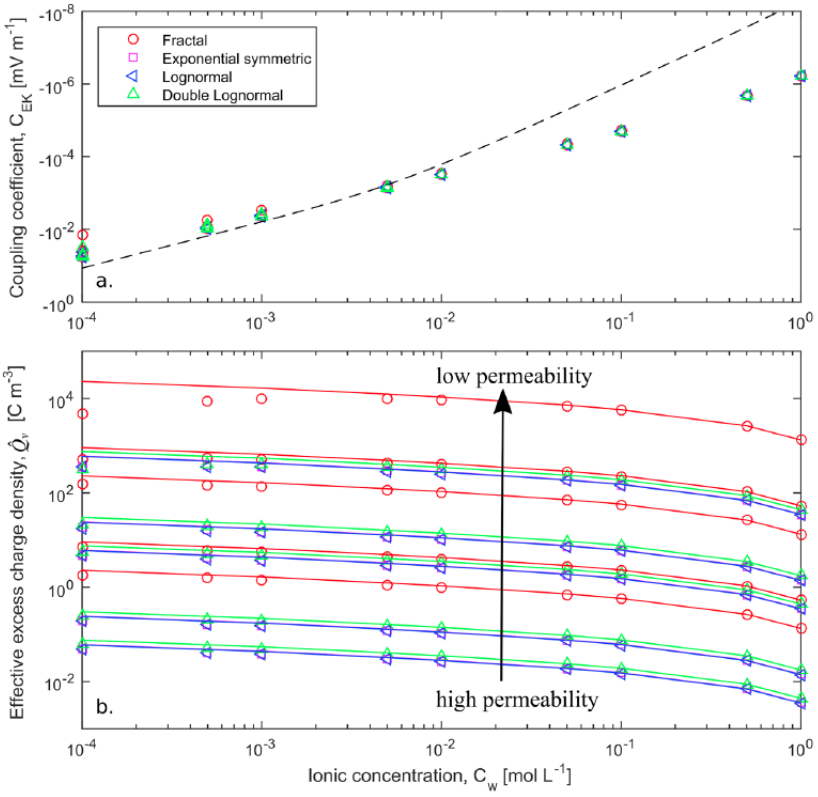

Figure 3.13: (a) Electrokinetic coupling coefficient and (b) effective excess charge density from the pore network simulations (from Jougnot et al., 2019).

a single capillary size. It takes into account the inertial term of the Navier-Stokes equation to explain both the dynamic permeability and the effective excess charge density dependence with oscillation frequency. Further work is needed to provide a more realistic model and apply it to seismoelectric simulations.

3.3 Towards a better characterization of field-scale hydrology and hydro-ecology through the use of SP in the critical zone

3.3.1 In situ SP monitoring of rainfall events

The use of the SP method to monitor rainfall infiltration can be tracked back to the pioneer work of Doussan et al. (2002). The authors proposed linear model to quantitatively link the SP signal measured in a lysimeter to the vertical Darcy velocity of the rainwater infiltration. However, since then, only few attempts have been made to pursue in this direction.

Revisiting literature data With the recent developments obtained from the flux-averaging approach, Jougnot et al. (2012) and later Soldi et al. (2019) tried to re-interpret the data of Doussan et al. (2002). Figure 3.14 presents the evolution of the effective excess charge with the saturation during five different rainfall event from the data. It shows that the flux-averaging approach seems to be able to reproduce the experimental data.

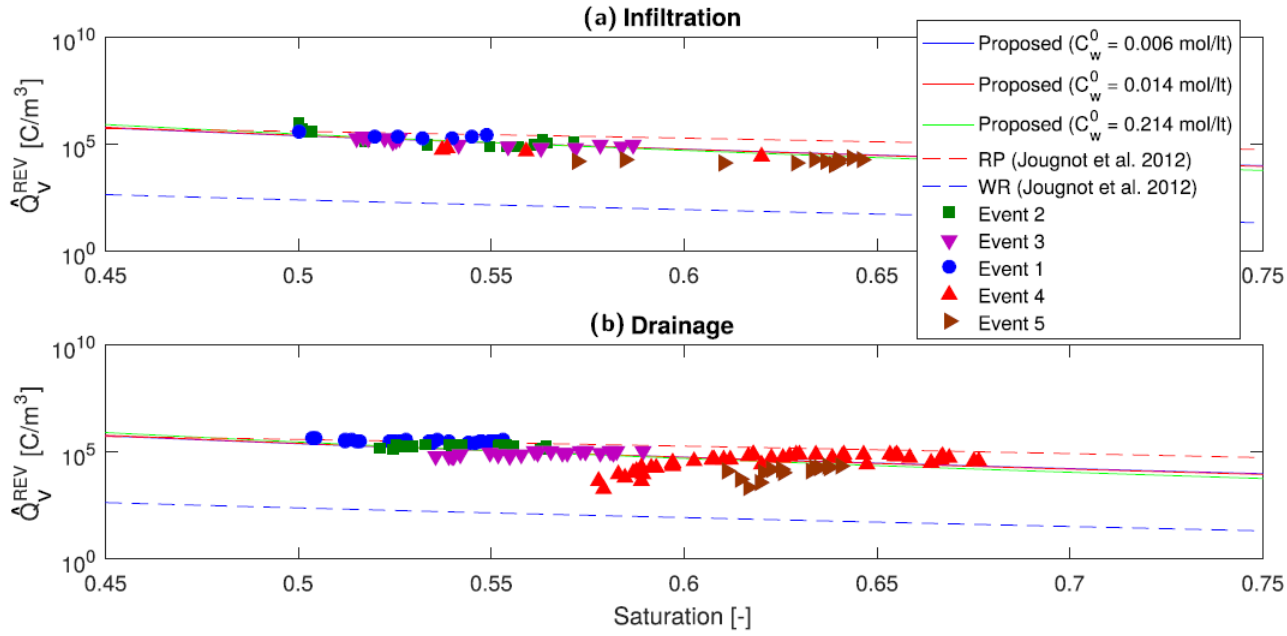

Figure 3.14: Effective excess charge density exctracted from the SP signal measured in Doussan et al. (2002) as a function of saturation during an (a) infiltation and (b) drainage phase of the event. Comparison of these data with the numerical WR and RP approaches of Jougnot et al. (2012) and the analytical closed form equation of Soldi et al. (2019) at three salinities (figure from Soldi et al., 2019).

Dedicated hydrogeophysical test site Jougnot et al. (2015) present a study about the use water infiltration monitoring by SP signal. We equipped the Voulund agricultural hydrogeophysical test site from the HOBE network in Denmark (Fig. 3.15a and b) with vertically distributed non-polarizable electrodes (Fig. 3.15c). This was the first work to focus on the vertical self-potential distribution prior to and during a saline tracer test. We build up a coupled hydrogeophysical modelling framework is used to simulate the SP response to precipitation and saline tracer infiltration.

The resulting model that compares favorably with electrical resistance tomography models is subsequently used to predict the SP response. The electrokinetic contribution (caused by water fluxes in a charged porous soil) is modeled by the flux-averaging approach from Jougnot et al. (2012) but with a

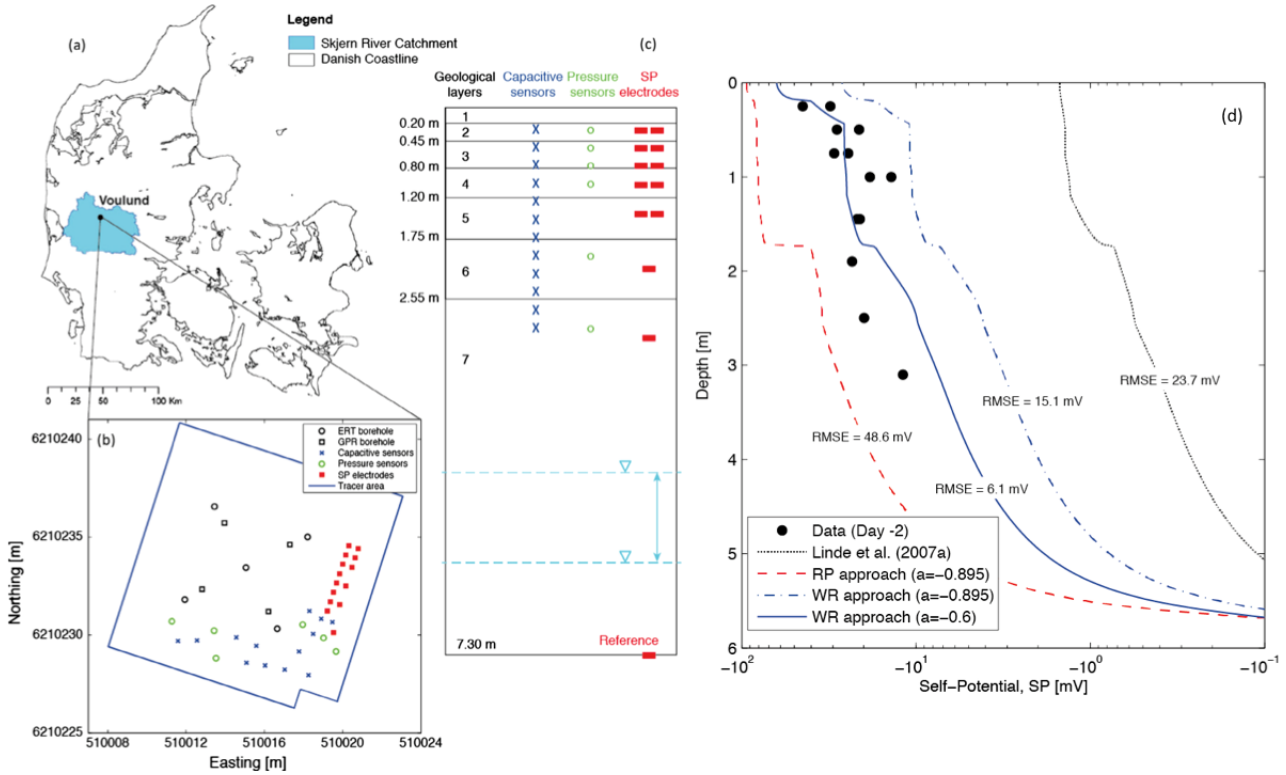

Figure 3.15: (a), (b), and (c) location of the Volund agricultral test site and lateral and vertical distribution of the instrumentation therein. (d) Measured and simulated SP signal as a function of depth prior to the tracer infiltration. Comparison between the prediction of the existing effective excess charge model from Linde et al. (2007) and the two approaches from Jougnot et al. (2012) (modified from Jougnot et al., 2015).

special focus on the effect of the pore water salinity on the effective excess charge density. Our results suggest that the effective excess charge evolution prior to the tracer injection is well described by the numerical model (Fig. 3.15d). Figure. 3.16 shows the results of the numerical simulations at four time steps before and after the saline tracer injection. After injection of the tracer the electrokinetic contribution decreases drastically (Fig. 3.16c) due to an increase of the medium electrical conductivity and an electro-diffusive contribution (caused by concentration gradients) needs to be considered (Fig. 3.16d).

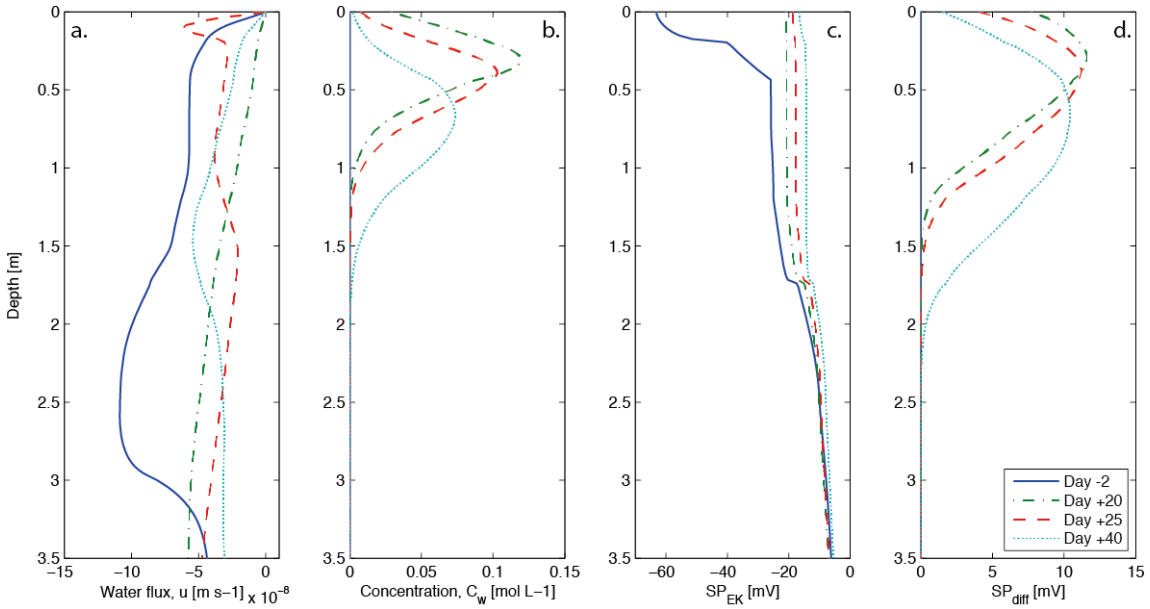

Figure 3.16: Numerical simulation of (a) the Darcy velocity, (b) tracer saline concentration, (c) SP electrokinetic and (d) electrodiffusive contributions as a function of depth before and after the saline tracer injection at the Voulund agricultural test site (from Jougnot et al., 2015).

3.3.2 In situ SP monitoring of root water up-take

The study of ecohydrology using geophysical methods is still an emerging topic, with only few works focusing on it (e.g., Mares et al., 2016). To the best of my knowledge, except for the pioneer work of Gibert et al. (2006) that performed a comparison of sap flow and daily electric potential variations in a tree trunk, no published works focused on the SP signals related to root-water up-take.

Voytek et al. (2019) therefore present the first study that collected SP measurements in a two-dimensional array at the base of a Douglas-fir tree (*Pseudotsuga menziesii*) in the H.J. Andrews Experimental Forest in western Oregon over 5 months (Fig. 3.17a). Fluid flow and electrokinetic coupling (i.e., electrical potential distribution) were simulated using COMSOL Multiphysics to explore the system controls on field data. The coupled model, which included a root-water uptake term, reproduced components of both the long-term and diel variations in SP measurements (Fig. 3.17b and c), thus indicating that SP has potential to provide spatially and temporally dense measurements of transpiration-induced changes in water flow (Fig. 3.18), therefore **opening up the possibility to use SP signal as input for ecohydrological models**.

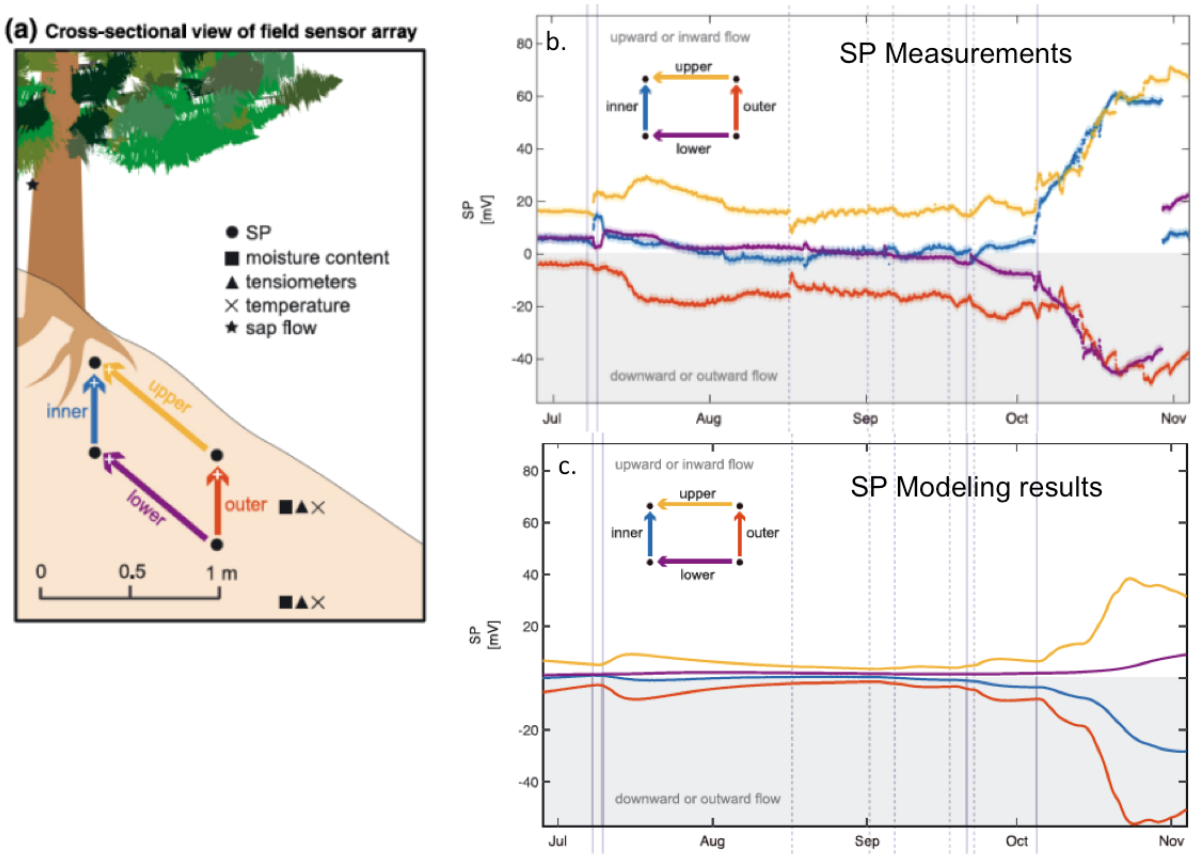

Figure 3.17: (a) SP monitoring set-up around the Douglas-fir tree at the in the H.J. Andrews Experimental Forest. (b) Measured and (c) simulated SP signals from eco-hydro-electrical coupled model (modified from Voytek et al., 2019).

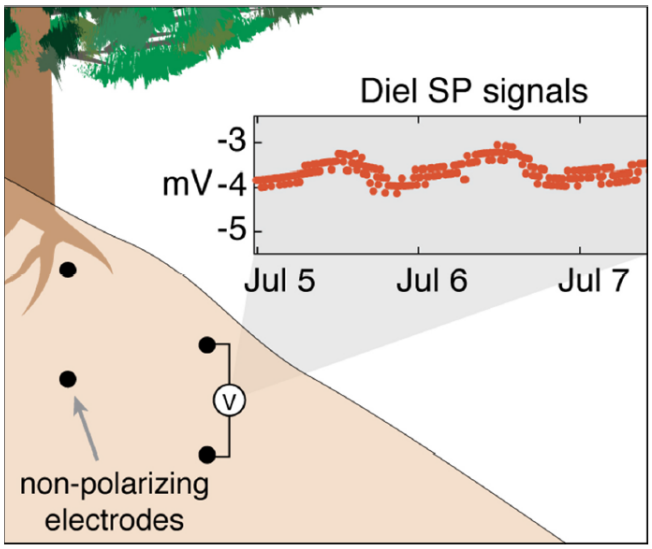

Figure 3.18: Evolution of the diel SP signal measured close to the tree roots (modified from Voytek et al., 2019).

Chapter 4

Fractures and fracture networks in porous media

Porous rocks often exhibit independent or connected fractures that can results from many different geomechanical processes (e.g., deformation, stress relaxation, dessication). These fractures and fracture networks present very contrasted properties in comparison to the rock background, therefore they can be very important mesoscopic heterogeneities affecting geophysical signal at the measurement scale.

In the context of resource extraction, the presence of fractures is generally considered to be an advantage as they facilitate access to materials stored in the matrix. Conversely, with regard to the storage of toxic elements, fractures represent a risk of leakage and subsequent migration of pollutants deep into the subsurface. Fracture characterization and fluid flow quantification in fractured media are two outstanding challenges, critically important in a wide variety of research fields and applications including hydrogeology, geothermal energy, hydrocarbon extraction, and the long-term storage of toxic waste.

In this chapter, I discuss the work we have done on two geophysical methods: seismoelectrics (section 2.1.3) and self-potential (section 2.1.2).

4.1 Effect of fractures on the seismo-electrical signal

4.1.1 Wave-Induced fluid flow in a fractured rock

The propagation of seismic waves through a medium containing mesoscopic heterogeneities, that is, heterogeneities having sizes larger than the typical pore scale but smaller than the prevailing wavelengths, can produce significant oscillatory fluid flow, generally referred to as Wave-Induced Fluid Flow (WIFF, Fig. 4.1), between the different regions composing the heterogeneous medium (e.g., Müller et al., 2010). The study of these WIFF can be done experimentally in well controlled laboratory conditions (see references in Müller et al., 2010) or numerically following the approach proposed by Rubino et al. (2009). WIFF can be one of the major sources of seismic attenuation in porous media.

Numerical study Among pioneer works, Rubino et al. (2013) showed that the presence of fractures and their orientation and connectivity strongly affect seismic signal due to the very strong compressibility contrast between the fracture(s) and the background. When the fracture is compressed by the pressure wave, the water that it contains is injected in the background, creating a WIFF and an associated energy dissipation (i.e., the Biot slow wave). This water flux, i.e. a relative displacement of water with respect to mineral, is expected to generate a streaming potential signal. Jougnot et al. (2013) propose, for the first time, that this phenomenon can be considered as an additional contribution to seismoelectric signals.

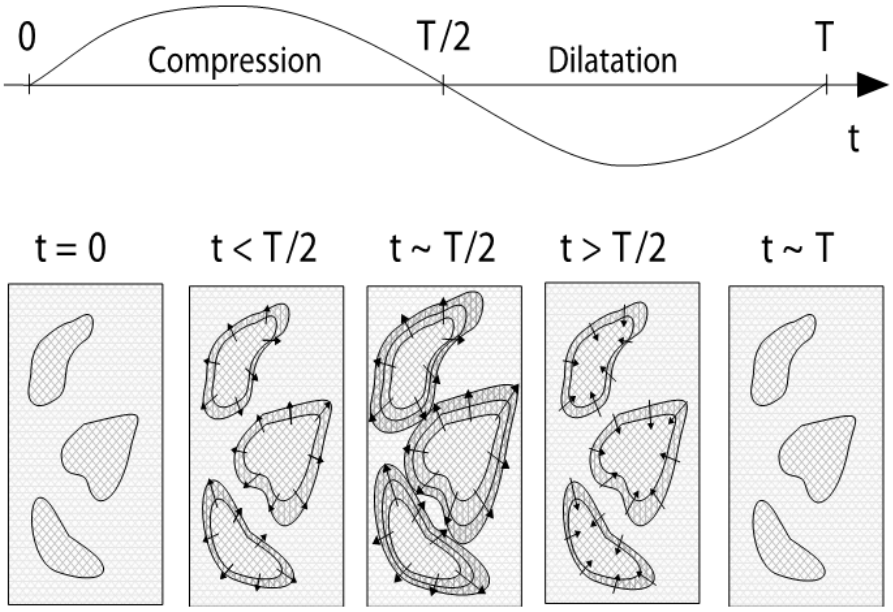

Figure 4.1: Illustration of the concept of Wave Induced Fluid Flow (from Müller et al., 2010). Arrows indicate the fluid flow direction.

Figure 4.2a presents the concept of the numerical oscillatory test as proposed by Rubino et al. (2009) and applied to a 2D numerical rock sample containing three discrete and unconnected fractures. A sinusoidal compression is applied at the top of the numerical sample and the poroelastic response of this medium is modelled by representing the mesoscopic fractures as highly compliant and permeable porous regions embedded in a stiffer porous matrix. The resulting relative velocity field of fluid is presented in Figs. 4.2b-e. At 1 Hz (Figs. 4.2b and c), the induced fluid velocity field is negligible. This is expected, as for such a low frequency, the diffusion lengths are larger than the size of the considered heterogeneities, and there is enough time during each oscillatory half-cycle for the pore fluid pressure to equilibrate to a common value. At a frequency of 10 kHz, the oscillatory compression produces a significant fluid pressure increase in the highly compliant fractures as compared to the stiffer embedding matrix, thus establishing an important fluid pressure gradient.

Figure 4.3 presents the WIFF contribution to the seismoelectric signals predicted from the relative fluid velocity fields obtained using the oscillatory compressibility test. Note that in this numerical test there is no wave propagation, therefore no co-seismic nor interface contribution (see section 2.1.3). Figure 4.3a and b show the magnitude of the electrical potential fields corresponding to the the relative velocity of Figs 4.2b-e for 1 Hz and 10 kHz, respectively. The magnitude and distribution of the seismoelectric signal strongly depends on the frequency of the applied compression. In particular, the fluid flow occurring in the vicinity of the fractures induces at 10 kHz measurable signal amplitudes of a few mV, while, at 1 Hz, the signal is too small to be measured. Note that these seismoelectric signals, like the relative velocities, are complex values that need to be characterized by amplitude and a phase that strongly depend on the oscillation frequency. Only amplitudes are shown here but a full description of values and phenomena can be found in the paper (Jougnot et al., 2013).

Given that the signal is directly dependent from the contrast between the mesoscopic heterogeneity and its background, additional tests were conducted for a wide frequency range using different background permeabilities. Figure 4.4 shows that the electrical potential measured at the top electrode is strongly frequency-dependent in terms of its amplitude and phase. The amplitude has a first peak at a frequency that depends on the background permeability, followed by a general increase at higher frequencies (Fig. 4.4a). The phase spectrum also shows a dependence with the background permeability, as the transition from high to low phase angles shifts to lower frequencies as the background permeability decreases (Fig. 4.4b). These spectral signatures are explained by the fact that

the frequency range where fluid flow prevails scales with the background permeability, together with the effects produced by the variations of the effective excess charge with the permeability (see section 3.10).

The magnitude of the seismoelectric signal is mainly governed by the compressibility contrast between the embedding matrix and the mesoscopic heterogeneities. Therefore, prominent seismoelectric effects are expected to arise not only in fractured media but also in partially saturated porous rocks. This in turn opens the perspective of developing seismoelectric spectroscopy as a novel method for characterizing such media.

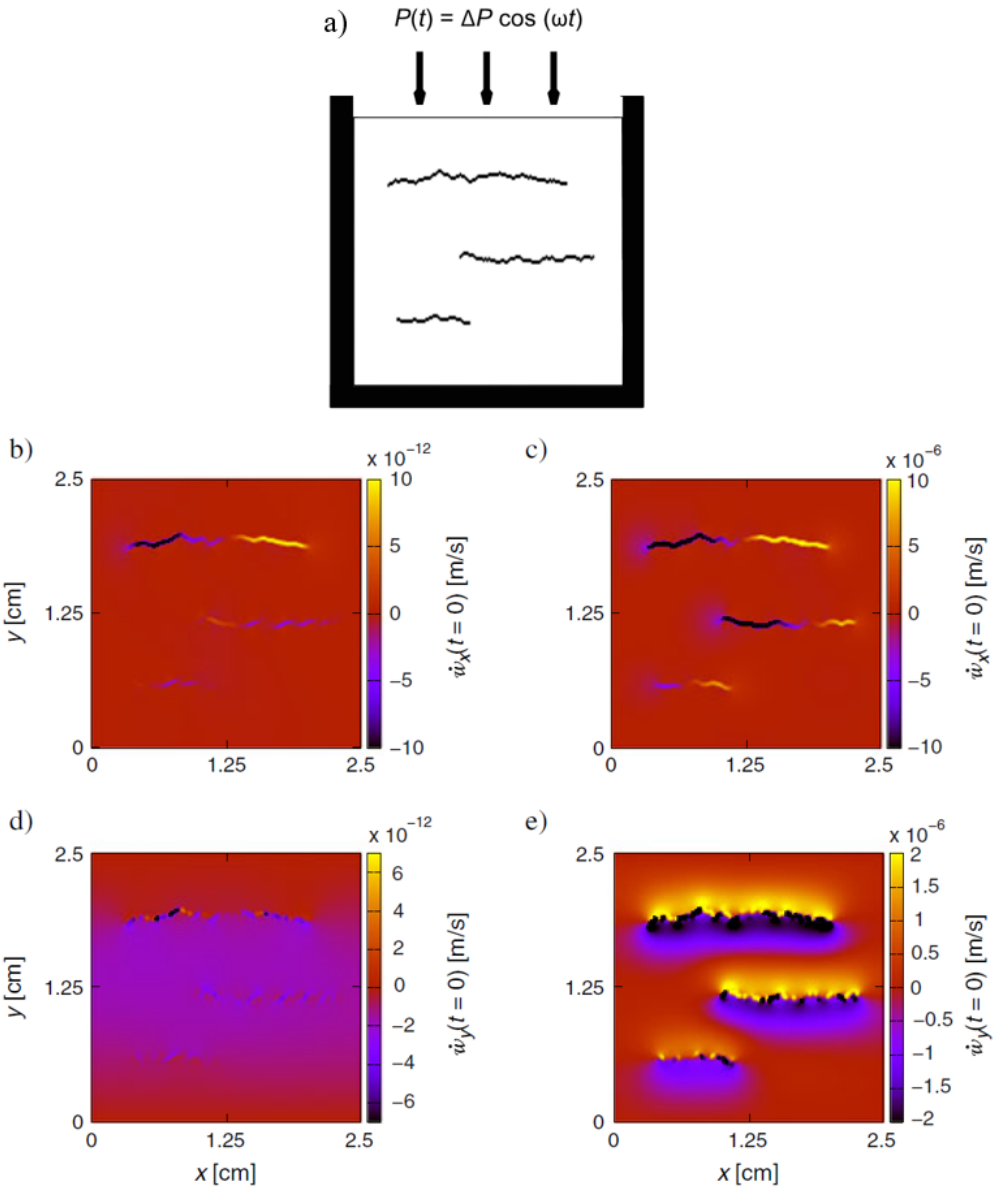

Figure 4.2: (a) Oscillatory compressibility test to simulate WIFF. Numerical simulation results for the (b and c) horizontal and (d and e) vertical components of the maximum relative fluid velocity field. The results correspond to an oscillatory compressibility test at the frequencies of (b and d) 1 Hz and (c and e) 10 kHz. Modified from Jougnot et al. (2013).

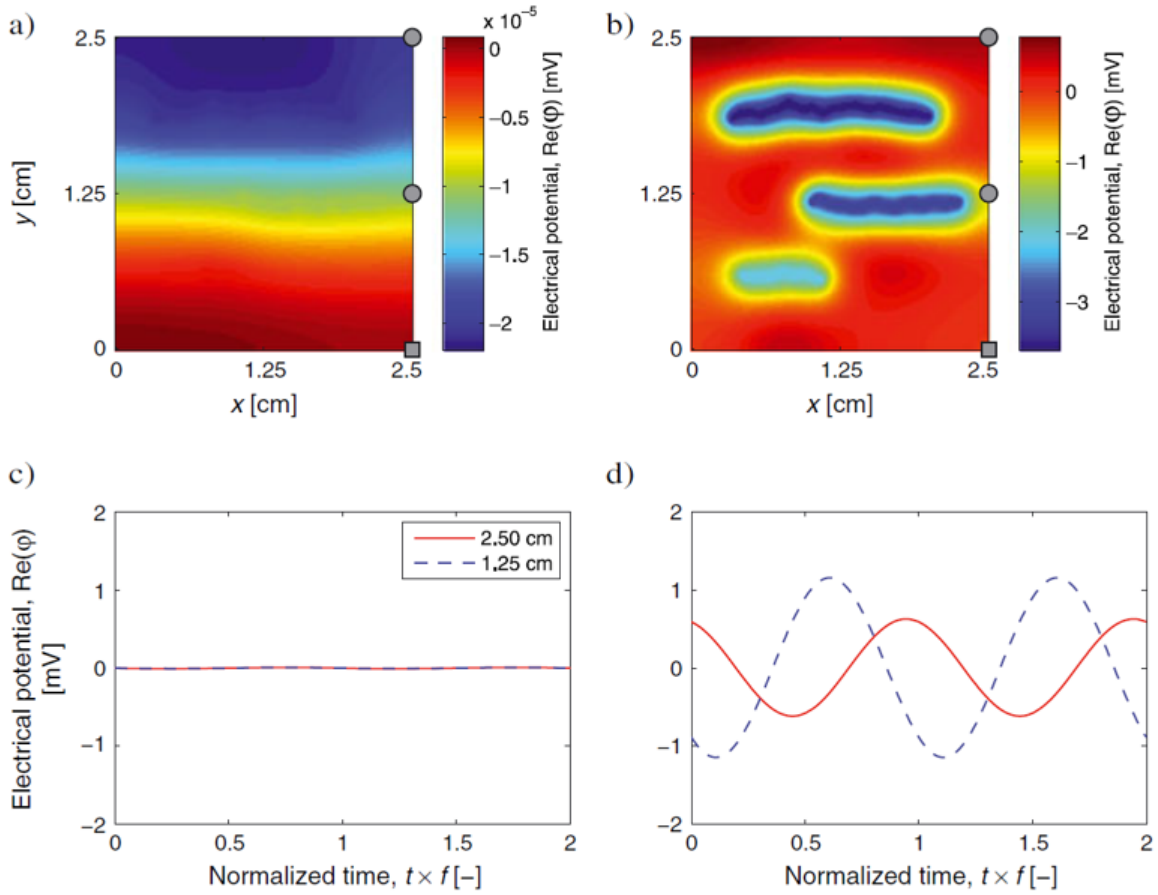

Figure 4.3: (a and b) Electrical potential distribution and (c and d) resulting electrical potential differences at two electrodes with respect to the reference electrode as functions of the normalized time. The grey square and the two circles (a and b) highlight the position of the reference and the potential electrodes, respectively. The results correspond to an oscillatory compressibility test at (a and c) 1 Hz and (b and d) 10 kHz (from Jougnot et al., 2013).

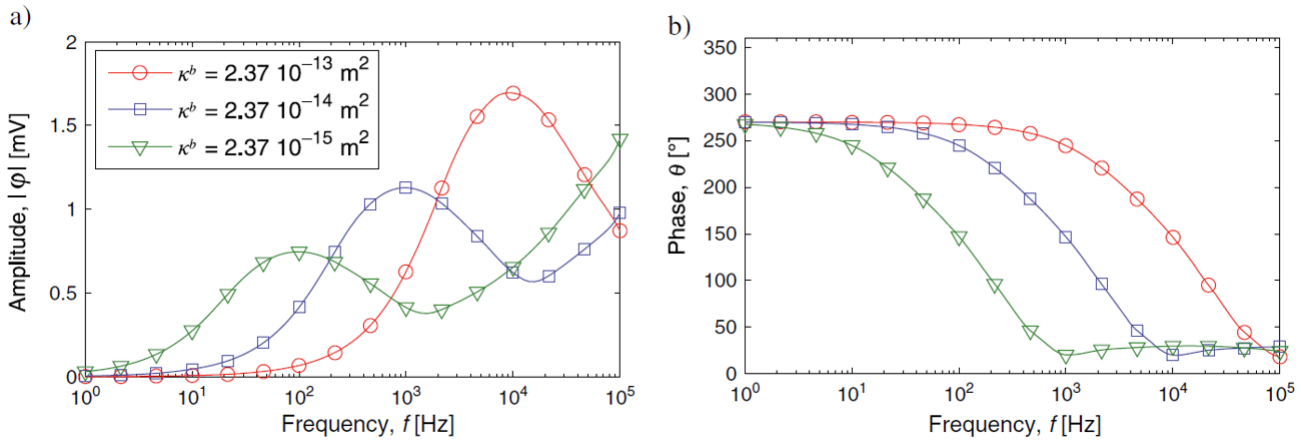

Figure 4.4: Effect of background permeability upon (a) the amplitude and (b) the phase of the electrical voltage recorded at the top electrode (y = 2.5 cm in Fig. 4.3) for different frequencies (from Jougnot et al., 2013).

Analytical study Given the strong dependence of these signals on the petrophysical and structural characteristics, we derived two analytical solutions to describe the seismoelectric response of a 1D rock sample subjected to an oscillatory compressibility test (Monachesi et al., 2015): first with a sample containing a horizontal layer at its centre (i.e., a general solution) and then for the particular case of a sample permeated by a horizontal fracture located at its centre (i.e., particular solution). Analyses of the general and particular solutions are performed to study the impact of different petrophysical and structural parameters on the seismoelectric response. We find that the amplitude of the seismoelectric signal is directly proportional to the applied stress, to the Skempton coefficient contrast between the host rock and the layer, and to a weighted average of the effective excess charge of the two materials. In presence of strong permeability variations, this frequency is rather controlled by the permeability and thickness of the less permeable material. The results of this study thus indicate that seismoelectric measurements can potentially be used to estimate key mechanical and hydraulic rock properties of mesoscopic heterogeneities, such as compressibility, permeability and fracture compliance.

4.1.2 Wave-Induced Fluid Flow in a fracture network

As presented above, the conversion of mechanical energy into electromagnetic energy is related to WIFF between the heterogeneities independent fractures and the embedding background. Rosas-Carbajal et al. (2019) propose the first study of this phenomenon on different fracture networks, highlighting the influence of the mechanical and hydraulic properties, as well as the geometrical characteristics, such as degree of fracture connectivity, of the probed medium on the resulting seismoelectric signal (Figure 4.5).

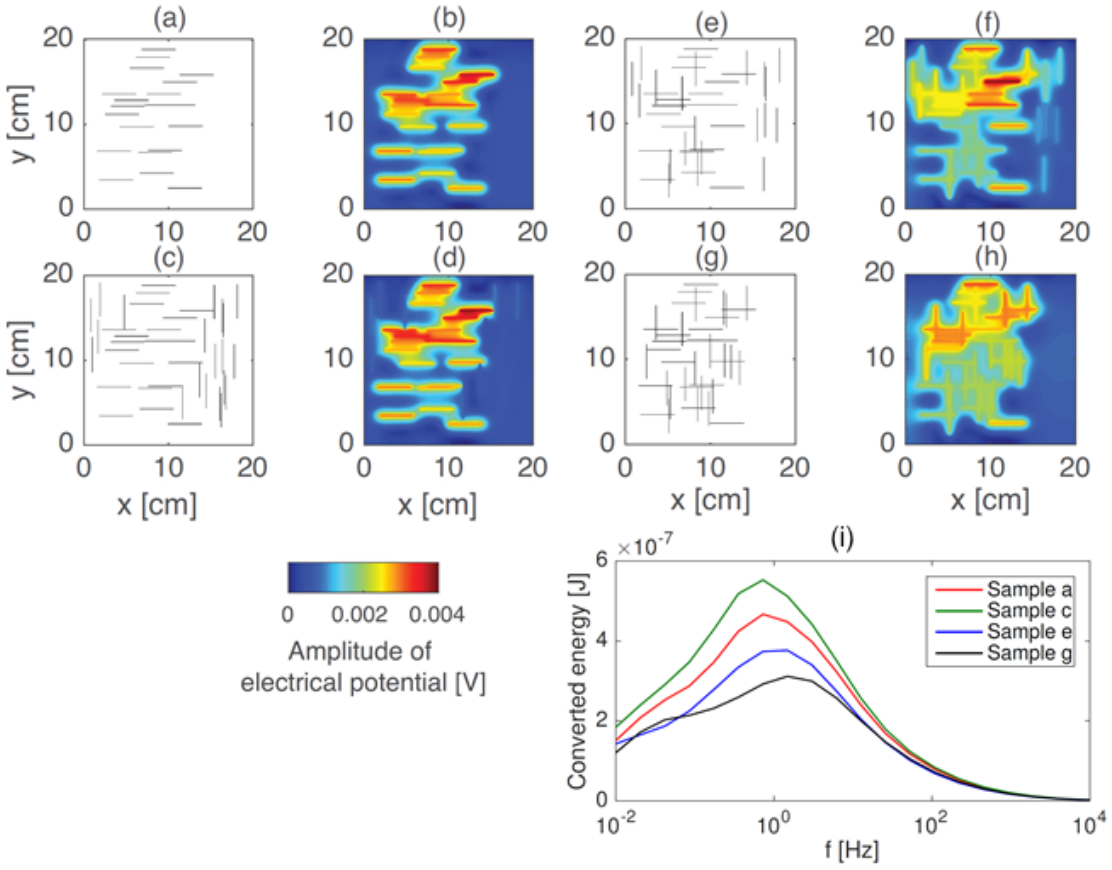

Figure 4.5: Numerical 2D rock samples used to test the effect of fracture connectivity on the seismoelectric signal: (a) sample containing horizontal fractures that are not connected between each other, (c) sample containing the same horizontal fractures as (a), plus vertical fractures, which are not connected to the horizontal ones, (e) sample containing the same amount of horizontal and vertical fractures as in (c) but with some of the fractures connected, and (g) same as (b) but with most of the fractures connected. (b, d, f, and h) Amplitudes of the electrical potential in the samples shown in the left column for a frequency of 0.73 Hz. (i) Calculated total energy converted to seismoelectric signals at the sample scale. Modified from Rosas-Carbajal et al. (2019).

In addition, we developed an energy-based approach to quantify the total energy converted to seismoelectric signals at the sample scale (Rosas-Carbajal et al., 2019). In particular, we apply our theoretical framework to synthetic models of fractured rock samples and study the spectral signature of the resulting seismoelectric signals. A clear dependence on fracture connectivity can be observed, as expected from Rubino et al. (2013). Adding the unconnected vertical fractures results in a higher seismoelectric energy, but as the fracture connectivity increases, there is a decrease in the total energy of the electric field. The peak frequency is also affected by the degree of connectivity. When the vertical unconnected fractures are added, the peak frequency does not change and corresponds to 0.73 Hz. Increasing the fracture connectivity shifts the peak frequency to higher values.

4.2 Streaming current generation in fractured network

The interest of the SP method to detect hydraulically active fractures and provide information about fracture properties has been highlighted by field evidences (e.g., Fagerlund and Heinson, 2003; Wishart et al., 2006). However, a lack of suitable numerical tools for modelling streaming potentials in fractured media prevents quantitative interpretation and limits our understanding of how the SP method can be used in this regard. Indeed, due to the strong contrast properties between the fracture and the matrix (i.e., background), solving the coupled hydraulic and electrical problem numerically is really computationally demanding and close to impossible in dense and complex fracture networks (e.g. DesRoches et al., 2017). In the present section, I will present the results of a numerical approach that we developed during the recent years.

4.2.1 The importance of the dual domain approach

To solve for the fluid flow and associated self-potential problems problems in fractured media, one can find two numerical approaches relying on a discrete representation of the considered fractures that are coupled to the matrix by using either the finite element method with adapted meshing (DesRoches et al., 2017) or the finite volume method within a dual-porosity framework (Roubinet et al., 2016).

The latter is a highly efficient discrete-dual-porosity (DDP) approach for simulating the coupled problem. It builds on the 2D electric current flow model developed by Roubinet and Irving (2014) and importantly considers the exchange of water between fractures and the surrounding matrix. The proposed modelling approach is specifically designed for highly heterogeneous fractured porous media that cannot be handled by standard numerical methods.

Roubinet et al. (2016) first tested the DDP approach to simulate field-scale SP experiments under pumping conditions for simple configurations for which a comparison can be made with standard finite-element methods (Fig. 4.6a). The DDP simulations are found to be approximately 50 times faster than standard finite-element methods (Figs. 4.6d and e).

The results of the validation (Fig. 4.6) provide important insight into whether it is reasonable to neglect matrix fluid flow when modelling streaming potentials in fractured media. As seen in Figs. 4.6b and d, making this assumption results in extremely small SP values compared to the case where matrix flow and matrix-fracture interactions are taken into account (Figs. 4.6c and e). This is despite the fact that in our example, the matrix permeability was set to be 8 orders of magnitude smaller than that of the fractures and thus the matrix can be considered as impermeable from a flow modelling perspective. Indeed, whereas extremely small matrix permeabilities are generally ignored for flow computations in fractured media, they cannot be neglected when modelling the SP response.

These results also imply that if the matrix material is strictly impervious or if the fracture network is so well connected that fracture-matrix fluid exchange is minimal, then the associated SP signals will be negligible. The results obtained for the case where matrix fluid flow was accounted for (Figs. 4.6c and e) also provide information concerning the sensitivity of the SP method to fracture-matrix fluid exchanges. As Fracture 2 does not intersect the domain boundaries (Fig. 4.6a), the fluid circulating in this fracture during the pumping experiment is provided by the surrounding matrix. As a result, the maximum value of is observed in the direction of Fracture 2 (Fig. 4.6e), which demonstrates that azimuthal SP measurements would be more sensitive to Fracture 2 than to Fracture 1.

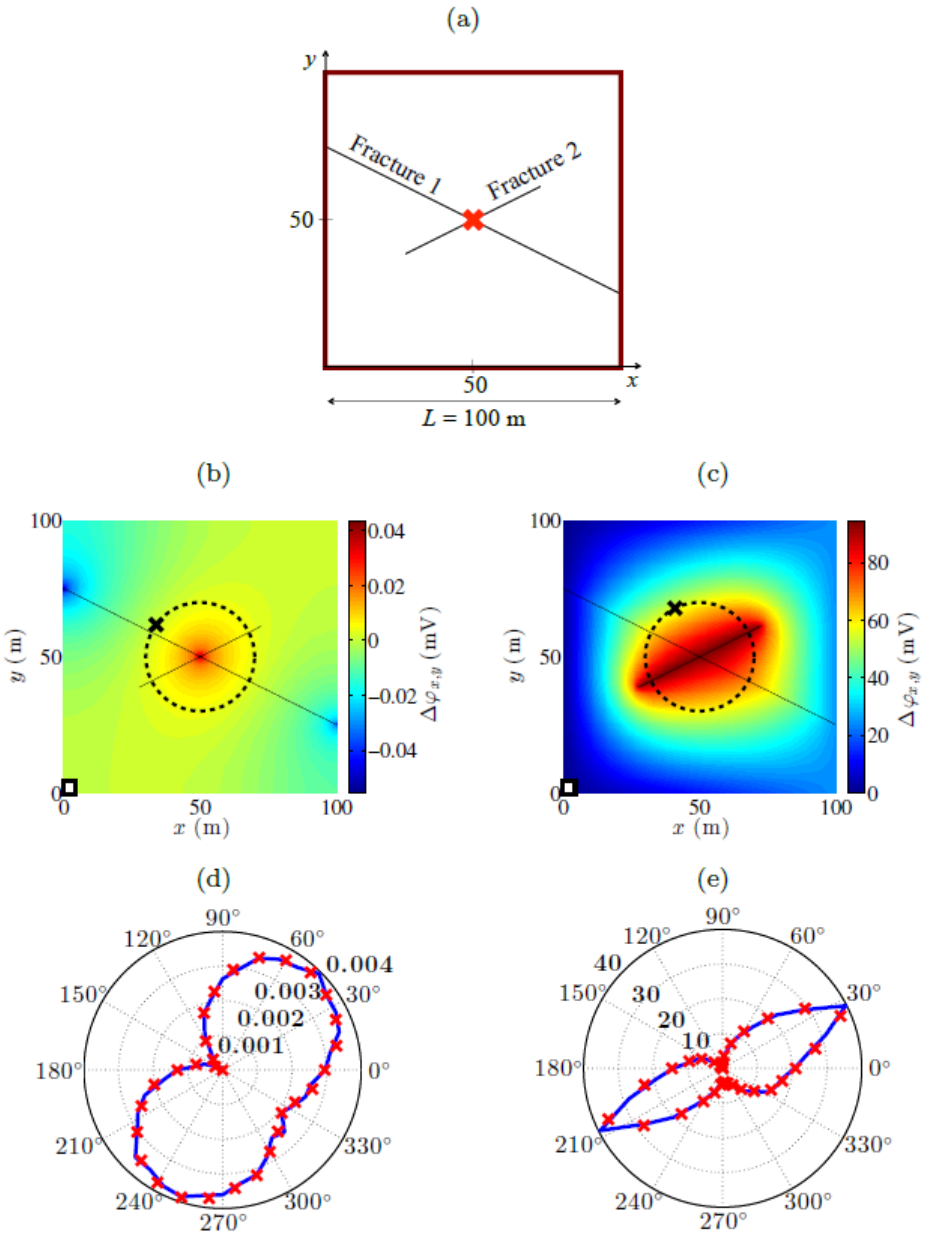

Figure 4.6: (a) Configuration used to validate the modeling approach of Roubinet et al. (2016) where the red cross represents the position of the considered pumping well. (b and c) Spatial distribution of the SP signal computed with the DDP approach where the white square represents the position of the reference electrode. (d and e) Polar plots of the SP signal with respect to a reference located at the black cross in b and c, respectively, and computed with the DDP approach (blue lines) and a finite-element solution (red crosses). Note that matrix fluid flow was ignored in b and d and accounted for in c and e (from Roubinet et al., 2016).

4.2.2 Fracture network and anisotropy

As shown in Roubinet et al. (2016), the sensitivity of SP to hydraulically active fractures is intimately linked with fracture-matrix fluid interactions. SP can detect individually the fractures that are hydraulically active for relatively small fracture densities. Indeed, for densely fractured media, we do not see any localized large values characteristic of dominant hydraulically active fractures having important fracture-matrix interaction, therefore no clear anisotropy appears in the simulated SP maps.

Figures 4.7a, b, and c show three examples of fractal fracture network models (see Jougnot et al., 2020). In these models, the number of fractures and the relative fracture lengths (i.e., the ratio of fracture to domain length) are defined from a fracture density, the smallest fracture length, and a fractal dimension. The positions of these fractures are randomly distributed with two possible angles with equal probability and the same aperture. Note that a deterministic fracture whose center is located at the domain center with a defined angle (represented in red in Figs. 4.7a-c), the pumping well is at the center of the domain.

These results show that a strong SP signal is observed for the primary fracture in which the pumping rate is applied when this fracture is not intersected by secondary fractures that are close to the pumping well (Figs. 4.7d and g). On the contrary, when the primary fracture is intersected by secondary fractures that are close to the pumping well and not connected to the domain borders, strong SP signals are observed at the extremities of the single secondary fracture (Figs. 4.7e and h) or the pair of secondary fractures (Figs. 4.7f and i). As demonstrated in DesRoches et al. (2017) and Roubinet et al. (2016), these results suggest that strong SP signals are associated with hydraulically active fractures, and that the largest values of SP measurements are related to important fracture-matrix exchanges.

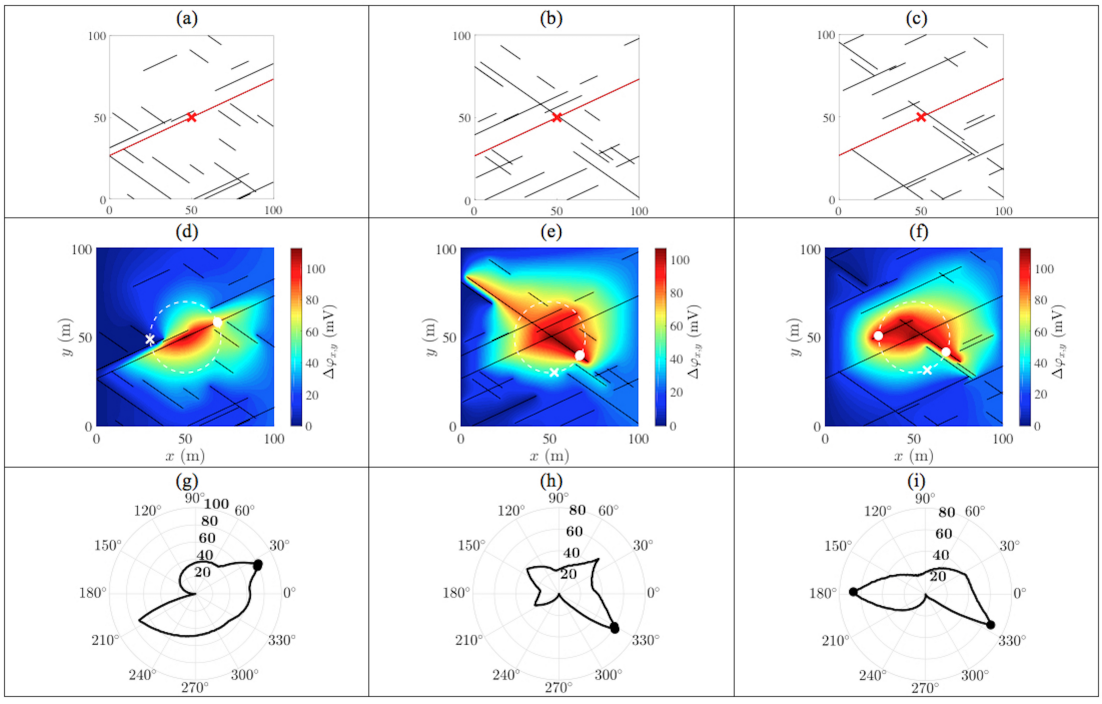

Figure 4.7: (a-c) Studied fractured domains where the red cross represents the position of the considered pumping well. (d-f) Spatial distribution of the SP signal with respect to a reference electrode located at position (x,y)=(0,0). (g-i) Polar plots of the SP signal along the dashed white circle plotted in (d-f) with respect to the minimum value measured along this circle and represented with a white cross. From Jougnot et al. (2020).

Chapter 5

Heterogeneities generated by transport and biogeochemical reactions

This chapter discusses heterogeneities that are not of physical nature (i.e, not only dependent from petrophysical properties of the rock) but depend on chemical or biological processes. These non-physical heterogeneities due to reactive transport and biogeochemical reactivity can induce physical properties contrasts that influence geophysical signals. I also consider these as mesoscopic scale heterogeneities as these reactivity are usually very localized but often larger than the pore scale.

The highly interdisciplinary topics that I'm going to address here are the subject of increasing interest. Most of them are part or go along with cutting-edge scientific research projects (e.g., European Research Council, French National Agency for Research).

5.1 Geoelectrical signature of reactive mixing

In subsurface hydrology, mixing processes occurring at interfaces between fluids of different chemical compositions play a key role in controlling the effective dilution rates of dissolved chemical species, as well as fluid-fluid and fluid-mineral reaction rates (i.e., mixing interfaces in coastal aquifers and hyporheic zones beneath rivers). Being able to understand, identify or quantify the reactivity biogeochemical of hot spots in the critical zone, is of tremendous importance.

Time-lapse geophysical imaging makes it possible to non-invasively and remotely track the motion and spatial distributions of tracers using surface- or borehole-based sensor deployments (e.g., Binley et al., 2015). Among the different methods, ERT and SIP have been used to monitor to biogeochemical processes and products.

5.1.1 Upscaling concept for the effective electrical conductivity

Inspired by the experimental set-up and results presented in Jougnot et al. (2018), Ghosh et al. (2018) propose to focus on the geoelectrical response of mixing-driven chemical reactions, for which the products are electrically more conductive than the background solution. A synthetic experiment is therefore set-up to investigate the impact of reactive mixing on the resulting effective electrical conductivity.

Figure 5.1a present synthetic set-up with a configuration in which reactive mixing takes place at the interface of two miscible fluids, one displacing the other. We consider the electrical conductivity produced by mixing fronts as defined over the Darcy scale. Since molecular diffusion alone is comparatively inefficient at mixing fluids, mixing rates in groundwater systems are primarily dictated by the coupling of molecular diffusion and velocity gradients that elongate mixing fronts and enhance concentration gradients. We compute the spatial distribution of the product concentration and analyse

its impact on the effective electrical conductivity. The transport equations are solved using the Lamellar Mixing Theory for a range of velocity gradients representative of the stretching rates experienced by mixing fronts in heterogeneous porous media (Borgne et al., 2014).

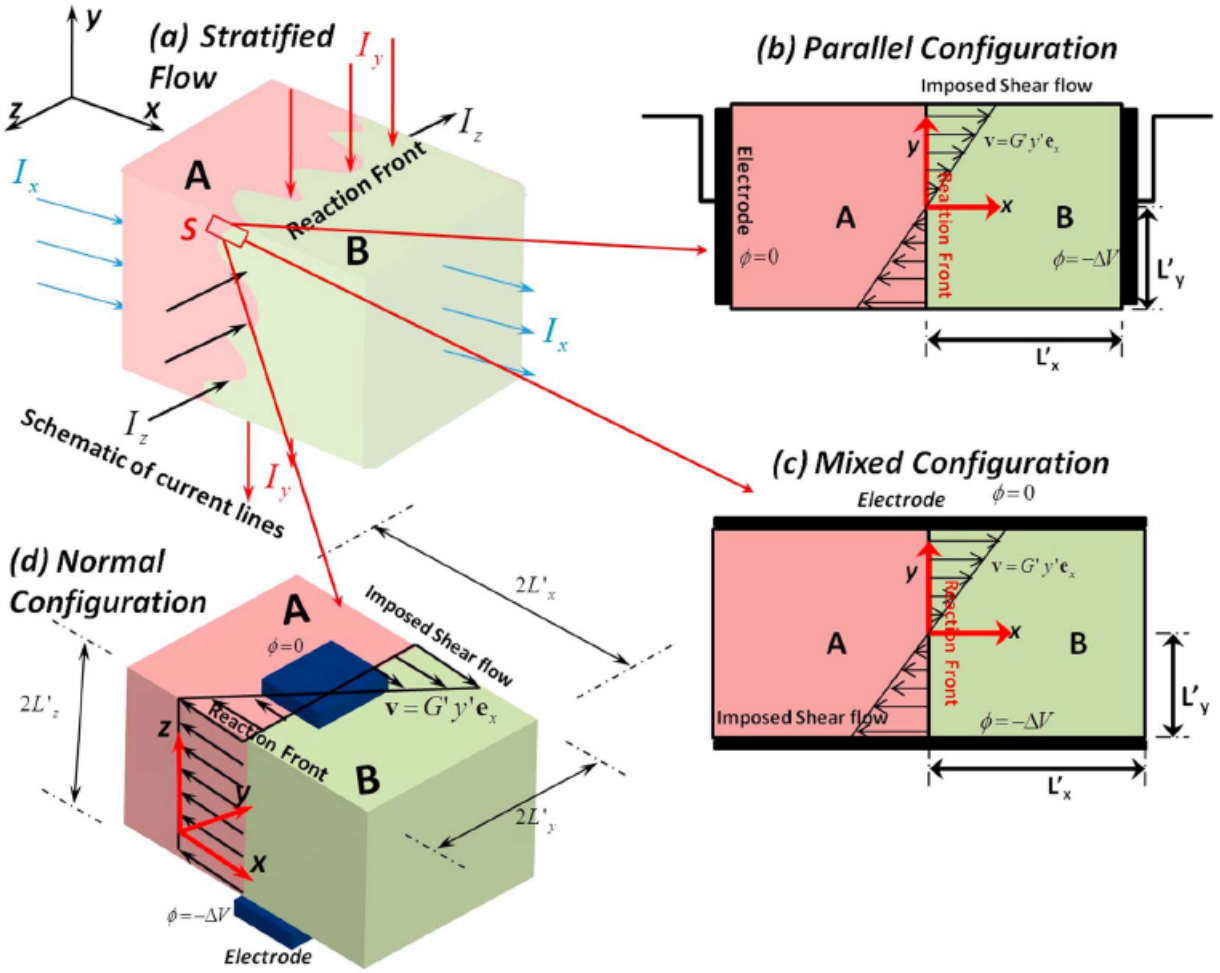

Figure 5.1: Schematic description of the system under consideration. (a) Stratified front between species A and B that can be considered as a superimposing individual shear flows. Based on the direction of the applied potential difference to simulate an electrical conductivity measurement with respect to the shear flow, the three studied are distinguished: (b) parallel configuration (i.e., parallel to the flow direction), (c) mixed configuration (i.e., perpendicular to the flow direction but parallel to the plane of shear), and (d) normal configuration (i.e., perpendicular to both the flow direction and the plane of shear) (from Ghosh et al., 2018).

To investigate the sensitivity of the effective electrical conductivity across the system under study to the reactive mixing dynamics, Ghosh et al. (2018) focus only on a simple shear unit. They assume that a uniform difference in electrical potential is applied across the domain of study, between two of its planar boundaries, opposite from each other. Depending on the relative orientations of this applied potential gradient, the flow and the plane of shear, we consider three different configurations: parallel, mixed, and normal configurations (Figs. 5.1b-d).

5.1.2 Effect of the transport properties

Figure 5.2 present the results of the modelling, i.e. the signature of reactive mixing at a single shear scale for a given set of transport properties. Figure 5.2a shows the temporal evolution of the net

change in effective conductivity, that is the difference from the initial conductivity, as a function of nondimensional time, while Figs. 5.2b, c, and d show the spatial distribution of the product concentration at different times.

Reactive mixing at the interface of the two reactants creates a highly conducting zone in the central part of the domain, surrounded by two regions of low conductivity. This band broadens as the reaction progresses. This induces a significant increase in effective electrical conductivity. It is interesting to note that due to stretching in the mixing process the spatial distribution of the product at different times yields strong differences between the electrical conductivity predictions of the three configurations, that is, a strong anisotropy (Figs. 5.2a).

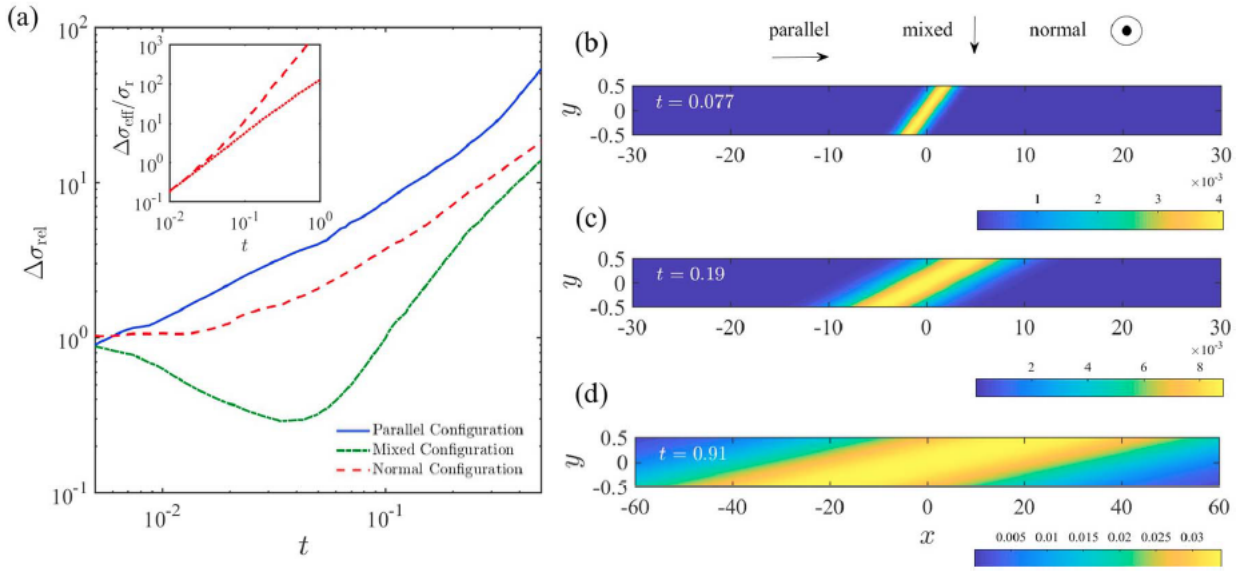

Figure 5.2: (a) Evolution of the relative change in effective conductivity with time, for the three configurations (i.e., its anisotropy). (b-d) Spatial distribution of product concentration (normalized by the initial reactant concentration) at three different times (from Ghosh et al., 2018).

To test the sensitivity of this idealized geoelectric response to the flow heterogeneity, the mixing rate, and the reaction kinetics, we analyse the effect of varying Péclet and Damköhler numbers (Fig. 5.3). These two dimensionless numbers are relevant to describe the transport and the reactivity. A high Péclet number indicate that the transport is more advective than diffusive (a null Péclet indicate no water flux), while a high Damköhler number indicates that the reaction is inherently fast compare to the diffusion process.

Figure 5.3 shows that the net change in effective conductivity is more pronounced for what we refer to as the mixed and normal configurations (Fig. 5.1). Our analysis shows that the different configurations may provide insights into different aspects of subsurface reactive mixing. Indeed, while the parallel configuration exhibits a high sensitivity to shear rate and, consequently, to the strength of the flow (as denoted by the Péclet number), as well as to the width of the reaction front, the two other configurations are more sensitive to the reaction kinetics, controlled by the Damköhler number.

This study was conducted on a highly idealized system and led to still very fundamental findings. However the development of millifluidic experimental set-up such as the one presented in Jougnot et al. (2018), would be a promising step forward that should be the subject of future scientific projects. Meanwhile, within the framework the ENIGMA ITN, one PhD project is dedicated to study transport properties (advection and diffusion processes) following the millifluidic approach that we proposed in section 3.1.

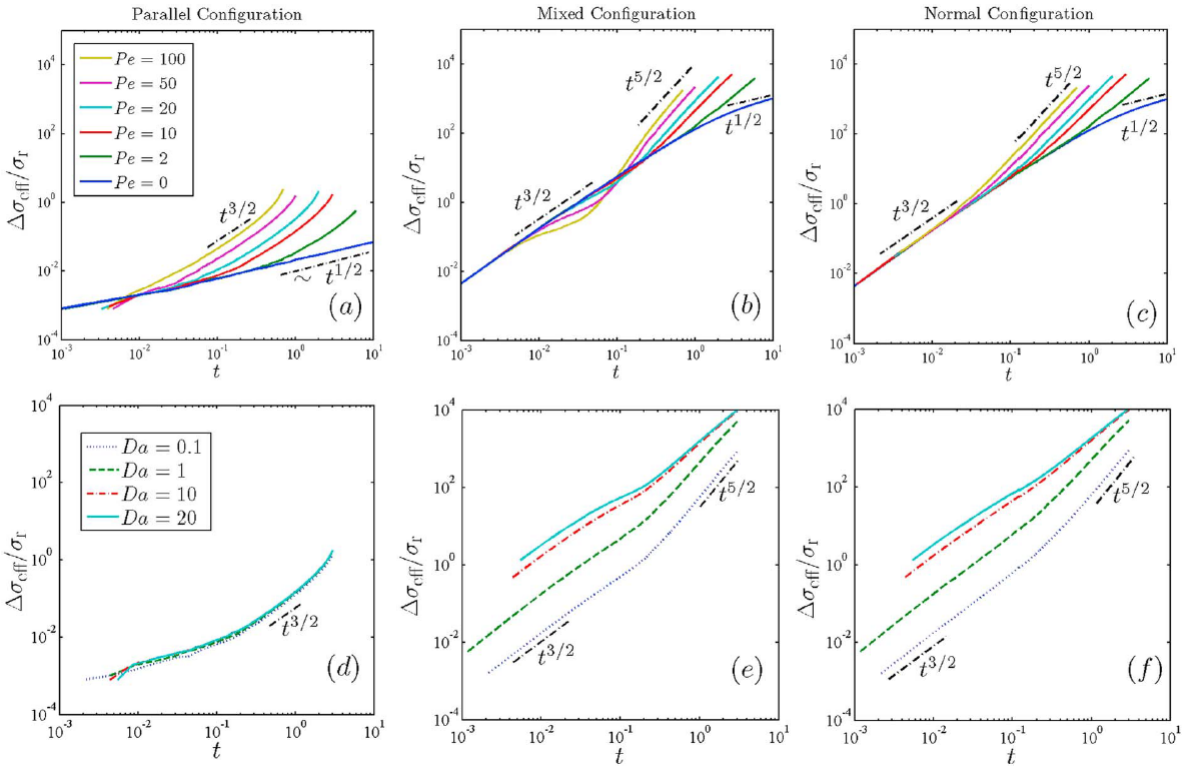

Figure 5.3: Effect of transport parameters on the effective conductivity for the three configurations: (a, b, c) Péclet (Pe) and (d, e, f) Damköhler (Da) numbers. For all cases, the effective electrical conductivity initially follows the trend observed in the absence of velocity gradients (Pe = 0) (from Ghosh et al., 2018).

5.2 SIP monitoring of carbonates dissolution and precipitation processes

Calcite is one of the most abundant minerals in the Earth's crust and one of the largest carbon repositories. Carbonate rocks are constituent of a large number of reservoirs (e.g., water, resources, geological storage) that are of societal (e.g., water supply) or scientific interest (e.g., critical zone studies).

Since calcite and other carbonate rocks are characterized by very high reactivity to the chemical properties of the surrounding water (pH, temperature, chemical composition, CO_2 partial pressure), they are subject to dissolution-precipitation processes is therefore of tremendous interest. Being able to monitor these processes with a non-intrusive geophysical method. Wu et al. (2010) showed the first experimental evidence that the complex conductivity method can be used to non-intrusively monitor calcite precipitation in porous media because of its sensitivity to the evolution of the mineralogy, pore structure and connectivity.

5.2.1 A new mechanistic SIP model for calcite polarization

The new SIP model proposed by Leroy et al. (2017) is based on the basic stern Model developed by Heberling et al. (2014). it describe the electrochemical properties of EDL (i.e., Stern and diffuse layers) of the calcite-water interface (Fig. 5.4a). Note that it is the same interface model as the one that we used in Li et al. (2016).

This new model is called mechanistic because it is based on the electrochemical properties of the EDL around particles. In order to be able to model the complex conductivity response of the calcite mineral, we approximate them as sphere (Fig. 5.4b) as an analytical solution exist for this geometry. Note that this is a strong but necessary approximation.

Our complex conductivity model considers (1) ion electromigration (conduction) in the diffuse layer (forming a dielectric medium around particles) and (2) ion electromigration and back-diffusion (i.e., polarization) of the discontinuous Stern layers around particles. The Stern layer polarization is compensated by the diffuse layer one following (Lyklema et al., 1983). This complex conductivity of a single particle is then upscaled at the REV scale using a Differential Effective Medium (DEM) scheme, providing a complex conductivity model for the calcite particle at the measurement scale.

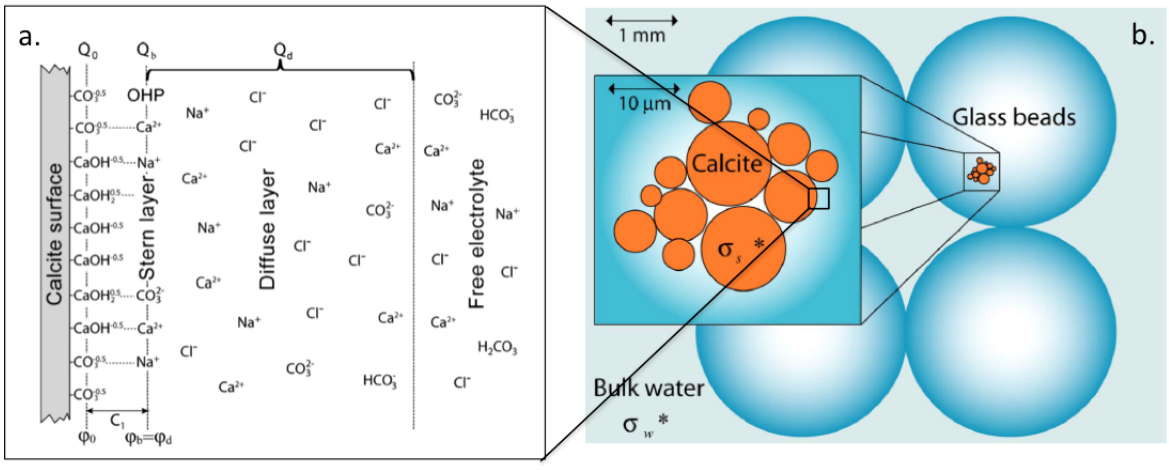

Figure 5.4: (a) Basic Stern interface model to describe the calcite-water interface (calcite (1 0 4) surface) when calcite is in contact with a NaCl and $CaCl_2$ aqueous solution at equilibrium with a pCO_2. (b) Sketch of the complex conductivity model of the experiment of Wu et al. (2010): precipitation of calcite on glass beads. Calcite particles that are mostly rhombohedral, are approximated as spheres. Modified from Leroy et al. (2017).

5.2.2 Modelling the calcite precipitation monitoring of Wu et al. (2010)

In order to test this new SIP model for calcite mineral, Leroy et al. (2017) propose a new interpretation of the experimental data of Wu et al. (2010). They performed complex conductivity measurements on a column packed with glass beads where they chemically induce calcite precipitation during 12 days. The SIP signal behaviour can be separated in two stage: before and during clogging (Fig. 5.5a and c). Due to their really small surface area and poor surface charge density, the glass beads polarization is negligible, as shown experimentally by Wu et al. (2010).

Figure 5.5 shows that the proposed surface complexation and complex conductivity models can successfully reproduce the experimental data (see the imaginary part of the complex conductivity Figs. 5.5a and c) by estimating the evolution of the calcite particle sizes and shape. The particle size can be estimated from the frequency at which the imaginary conductivity is higher (i.e., the peak frequency): larger particles tend to polarize slower, therefore at lower frequencies (Figs. 5.5b and d). The particle shape can be inferred from the cementation exponent (Fig. 5.6).

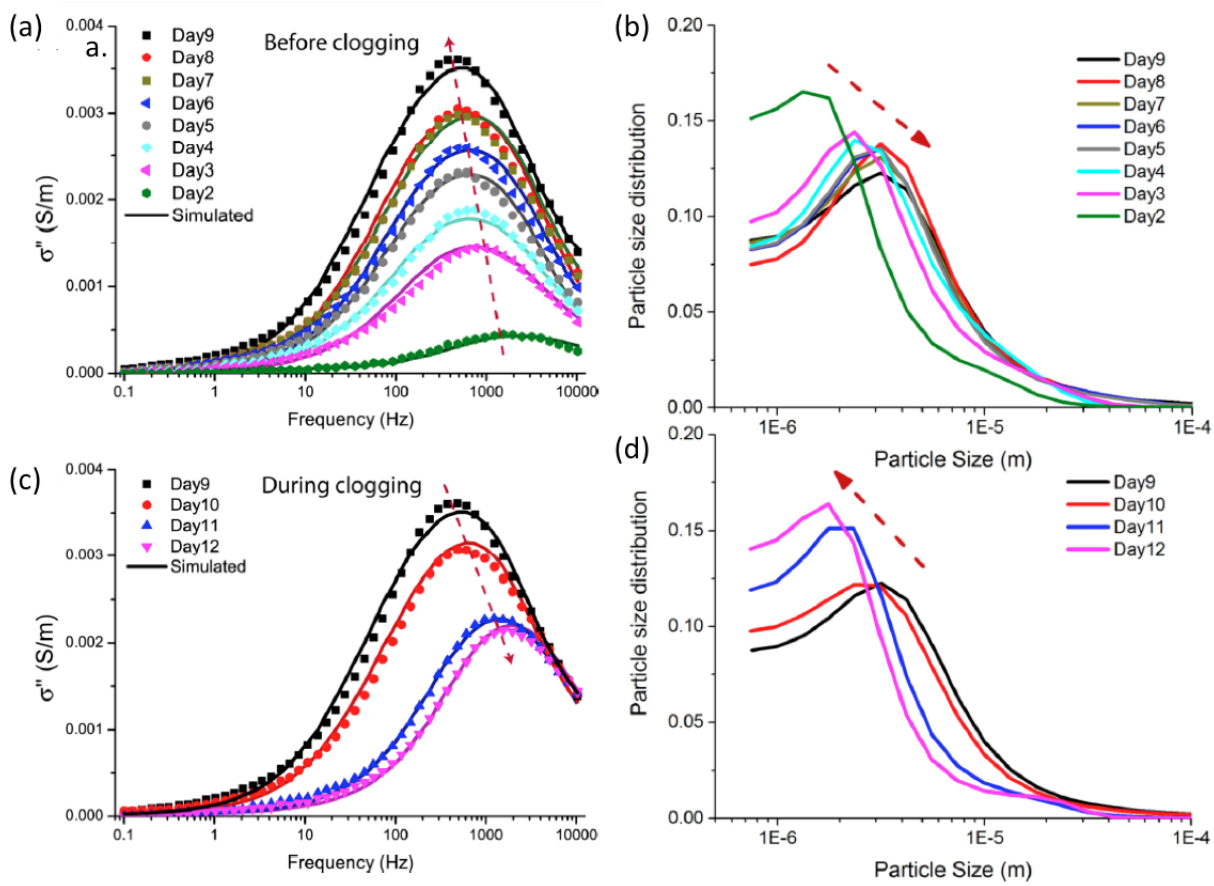

Figure 5.5: Imaginary conductivity spectra of calcite precipitation on glass beads as a function of time in days (a) before and (c) during the pore clogging by the calcite precipitate. Imaginary conductivities inferred from the complex conductivity model are represented by the lines and the symbols represent the imaginary conductivity measurements of Wu et al. (2010). (b) and (d) evolution of the computed calcite particle size distribution of during calcite precipitation corresponding the model of (a) and (c), respectively. Modified from Leroy et al. (2017).

From our modelling results, we can propose an explanation for signal evolution seen in Wu et al. (2010). At the early stage of the calcite precipitation experiment, the particles sizes increase and particles flatten with time because calcite crystals nucleate at the surface of glass beads and grow into larger calcite grains. At the later stage of the calcite precipitation experiment, modelled sizes and cementation exponents of calcite particles decrease with time because large calcite grains aggregate

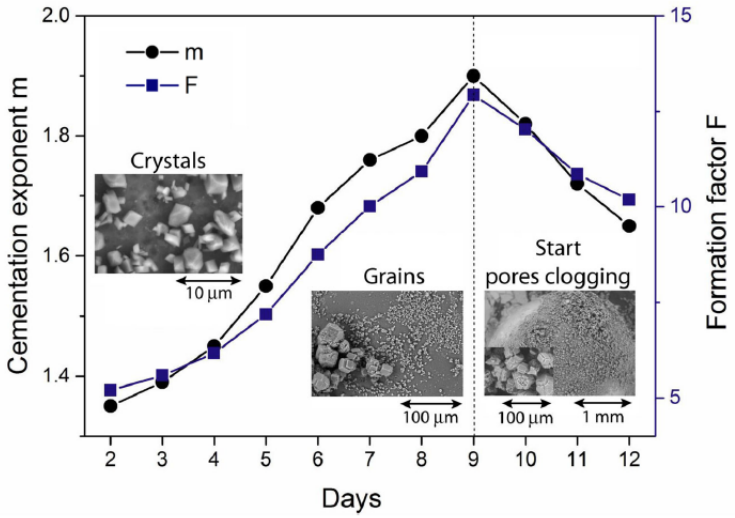

Figure 5.6: Computed particles cementation exponent (m) and formation factor (F) changes during the calcite precipitation experiment of Wu et al. (2010). The cementation exponent and formation factor of the glass beads pack where calcite precipitation occurs have a different trend of changes before and after the starting of the pore clogging (day 9) (from Leroy et al., 2017).

(pore clogging) over multiple glass beads and only small calcite crystals polarize. These findings are corroborated by microscopy imaging (pictures on Fig. 5.6).

If the proposed model seems to be able to explain well the experimental data, many open questions remain regarding the geoelectrical signatures of carbonates. Within the framework the ENIGMA ITN, one PhD project is to study the effect of effects of the water solution composition on the spectral induced polarization signals of calcite precipitation. Following the millifluidic approach described in Jougnot et al. (2018), calcite precipitation monitored with SIP and a high-resolution camera to relate the signals to the cristal growth kinetics. I am also supervising a PhD thesis dedicated on monitoring the dissolution processes with SIP and SP signals, the experiments are in progress.

5.3 Biogeophysics, the next frontier

These last two decades, the development of biogeophysics studies have confirmed the potential for geophysical techniques to measure not simply the physical and chemical properties of the sub-surface, as already well established, but also to detect microbial activities, thus representing a major paradigm shift in geophysical thinking (Atekwana and Slater, 2009).

5.3.1 Geophysical signatures of bioremediation processes

Bioremediation in contaminated soils involves both microbial activities and chemical reactions, it is therefore a perfect object to explore the potential of biogeophysics. This is pretty clear given the number of studies showing the possibility to monitor biogeochemical activities using geophysical methods (e.g., Atekwana and Atekwana, 2010).

In the literature, several sets of data have shown the possibility to monitor biogeochemical activities using electrical methods through changes in real and quadratic electrical conductivity spectra (e.g., Werkema Jr et al., 2003) and redox reactions (e.g., Revil et al., 2010). Fewer works have studied the evolution of mechanical properties under the effect of bacteria and biofilms (e.g., Davis et al., 2010), especially on the shear modulus (Atekwana, personal communication). Some studies also explored the link between magnetic susceptibility and SIP for hydrocarbon polluted samples but not in the context of remediation (e.g., Mewafy et al., 2011). However, when used individually, geophysical methods can lead to mis-interpretations or multiple solution problems. For example, in bioremediation context, a decrease in the electrical conductivity could be due to a decrease of the water saturation replaced by air or oil, or even to pore-clogging effects due to biofilm development. In this particular case, mechanical measurements would help to better constrain the process in place as the presence of oil or air in the medium results in very different acoustic-wave velocity.

In the GeoProcesS project, started in 2018 and funded by the City of Paris, I chose propose to a multi-method monitoring of hydrocarbon contaminant bioremediation to better understand and better constrain the processes occurring in the near-surface. The range of methods that we propose covers the entire spectrum of physical properties described by the review proposed by Atekwana and Atekwana (2010): electrical, electromagnetic and mechanical properties and are complemented by state-of-the-art biogeochemical characterization (Fig. 5.7). A multi-method approach, allowing the measurement of all physical properties at once, is, to my opinion, the way to tackle such a multidisciplinary problematic.

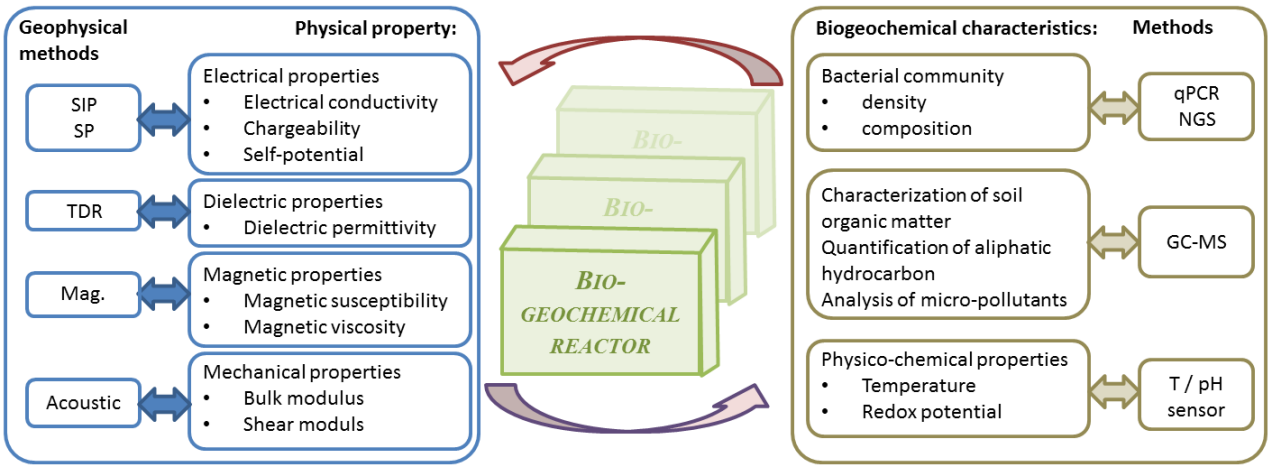

Figure 5.7: Sketch of the proposed approach for the GeoProcesS project: coupling geophysical and biogeochemical methods to study bioremediation processes.

We expect that the comparative study of physical properties and biogeochemical characteristics

and their careful monitoring will provide a really exhaustive dataset of bioremediation monitoring. This dataset will be used for the theoretical part of the study presented below and later shared with the scientific community through the submission of a data-driven paper.

5.3.2 Toward a hydro-bio-geophysical approach of the critical zone

If contaminated areas show a particularly strong biological reactivity, the GeoProcesS trans-disciplinary project is a first step for which biogeophysical monitoring is expected to work. Highly valuable outputs could also be found in other environments where the development of microbial biofilms is particularly marked and of ecological interest (Flemming et al., 2016), such as riparian areas and other ecotones or root zones where contaminant transport and transformation are particularly active. The final aim of the proposed approach is to apply geophysical tools and previously developed models to the study biogeochemical reactions on the various compartments of the critical zone (Fig. 5.8): **a hydro-bio-geophysical approach of the critical zone**.

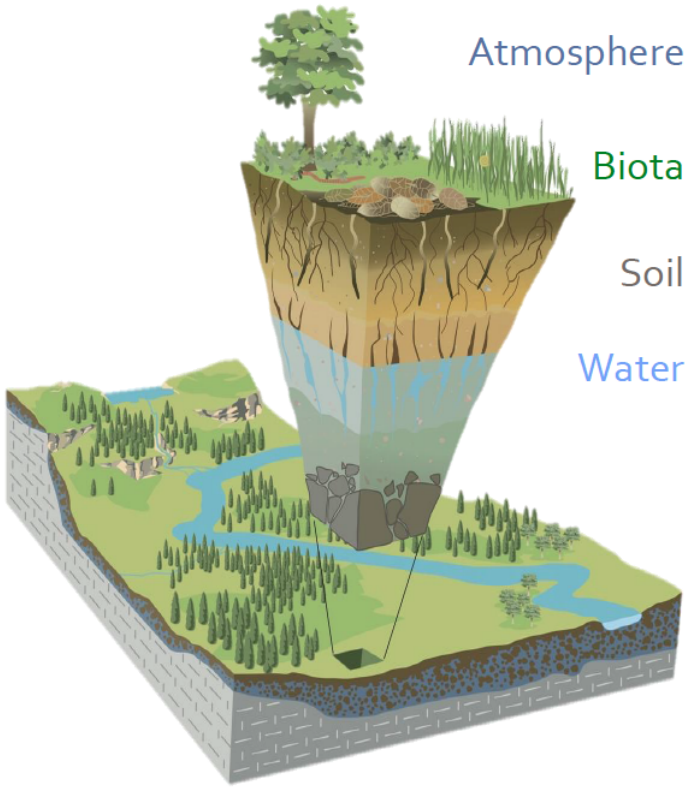

Figure 5.8: Sketch of the different compartments in the critical zone (from Chorover et al., 2007).

Chapter 6

Partial conclusions and scientific perspectives

Since the defence of my PhD thesis I had the opportunity to pursue my research on the development of the geophysical methods for environmental studies. The main scientific question I am trying to address is related to the heterogeneities appearing at a scale that can be defined as mesoscopic, that is, larger than the pore scale and smaller than the geophysical method measurement scale.

In the present document, I distinguish three main types of mescoscopic scale heterogeneities: the effect of the water distribution in porous media related to the pore size distribution, the presence of fractures, and the biogeochemical reactivity in the near surface.

Over the last ten years, my research has been evolving from hydrogeophysics of the vadose zone to a larger and more integrative use of geophysical methods to characterize the critical zone. If most of my research are based on theoretical developments and laboratory experiments, I started to apply these results to field scale studies. This is a research objective that I intend to keep and develop by taking advantage of the OZCAR test sites and the CRITEX equipments. With the numerous progresses in the different critical zone sub-communities, it becomes possible to move toward more and more integrated and trans-disciplinary research.

Given the multiplicity of scientific disciplines that are needed to better understand the critical zone, collaborative projects are, in my opinion, the most effective way to make progress. Therefore, I am leading and participating to a number of on-going research projects that will allow me to pursue my researches in the following years.

ENIGMA ITN As mentioned in the introduction, I am the deputy coordinator the Innovative Training Network ENIGMA (European training Network for In situ imaGing of dynaMic processes in heterogeneous subsurfAce environments) funded by the European Commission. ENIGMA ITN aims at training a new generation of young researchers in the development of innovative methods for imaging process dynamics in subsurface hydrosystems, in order to enhance understanding and predictive modelling capacities and to transfer these innovations to the economic sector. The 15 young future PhD students will contribute to develop the spatial representation of subsurface heterogeneity, fluxes, chemical reactions and microbial activity, through the integration of data and approaches from geophysics, hydrology, soil physics, and biochemistry. The network ENIGMA gather 21 partners (15 academic and 6 industrial) from 8 European countries. Each of the 15 future PhD students are conducting their research work in 2 or 3 institutions, in collaboration with the industrial partners. Started in January 2017, the Enigma ITN will run until December 2020. I am related to several PhD projects and officially co-supervising the PhD thesis of Lara Blazevic that focuses on the spatio-temporal monitoring of water redistribution in the subsurface with seismic methods.

CIFRE EDF As mentioned in the present document, the use of various complementary geophysical techniques is an efficient way to decipher complex processes. In the framework of a CIFRE project with EDF (Electricity of France company), the project "Coupling geophysical methods for reconnais-

sance survey and monitoring of dams' integrity" aims at using data mining algorithms to improve our ability to image the near surface through the use of various geophysical techniques. This project started in 2017 and is jointly funded by ANRT and EDF. It funds the salary of a PhD student, Kawtar Sabor, whom I am co-supervising.

ANR ExCITING In the continuity of my former PhD thesis topic, I am also co-PI of a Collaborative Research Project funded by ANR that we called ExCITING (EXploring geological resourCes and reservoir Integrity by geophysical prospecTING of clay properties from nano to field scale). The main objective of the project is to improve the characterization of the complex and frequency dependence of electrical properties of different clays minerals and mixtures. The project combines measurements, modelling, and inversion tools at different scales (from nano to pluri-metric scales) in parallel to instrumental development. It requires the development of upscaling procedures, from the mineral-water interface (nano-micrometric) to the field scale (decametric to kilometric). The project started in 2018 and will run until 2021. It involves five main scientific partners and two PhD students. I am co-supervising the PhD project of Aída Mendieta that focuses on an experimental and numerical study of SIP signatures of the different clay minerals.

EC2CO STARTREK The project STARTREK (Système péTrophysique de cAractéRisation du Transport Réactif en miliEu Karstique: Petrophysical system to characterize reactive transport in karstic media) funded by the CNRS for 2018 and 2019 regroups two french universities. The main purpose of this project is to better understand the dissolution of carbonate material by the monitoring of its petrophysical properties. I am co-supervising the PhD project of Flore Rembert that aims at developing geoelectrical methods (SIP and SP) for the monitoring of dissolution-precipitation processes in carbonates.

GEOPROCESS In December 2017, I received a grant from Paris City - Emergence Research Grant, to create the trans-disciplinary research team GeoProcesS: GEOphysical monitoring of hydrogeological and bio-geochemical PROCESses in contaminated Soils. The GeoProcesS team is hosted by UMR 7619 METIS at Sorbonne University, and regroup 6 permanent researchers (from geophysics, geochemistry and microbiology) and one PhD student. The research project associated to this team aims at merging geophysical and biogeochemical expertise to support the development of existing techniques for the qualification and remediation of contaminated sites. The main goal of the team is to conceive an integrated use of geophysical methods for the quantitative study of the effectiveness of chemical and microbiological reactions occurring during remediation processes of contaminated soils and sites. I am co-supervising the PhD thesis of Karim Bezzaouya working on this topic. Started in December 2017, GeoProcesS will run at least until November 2021, but we intend to use it as a seed to grow larger projects.

All these on-going collaborative projects are very complementary in themes and methodology but they all are structured around the three research strategies that I have used since the beginning of my academic carrier: theory developments, laboratory experiments, and field measurements. In the future, I will pursue the development of new theoretical models, coupling different physics in order to develop new petrophysical relationships. Indeed, it is a critical point that still need a lot of research to address: relate geophysical measurements to the properties of interest. The laboratory component of my approach is clearly complementary and is needed: perform high quality experiments in well-controlled conditions to test the proposed new theories. Then, last but not least, going to the field to confront the findings we obtain on simple ideal systems to the intrinsic complexity of field scale. This last point is the one that I need to develop the most in the future.

I believe that multidisciplinary research projects (ongoing and future ones) pave the way to a deeper exploration of many fundamental issues that we need to address to better understand the criti-

cal zone. Therefore I believe that developing an integrated hydro-bio-geophysical approach will contribute to address the three large scientific questions as defined in section 1: (1) how can determine and monitor the the architecture of the Critical Zone ? (2) how to decipher the hydro-biogeochemical processes taking place in the critical zone ? and (3) how can we predict the future of the critical zone?

Bibliography

de Anna, P., Jimenez-Martinez, J., Tabuteau, H., Turuban, R., Le Borgne, T., Derrien, M., Méheust, Y.. Mixing and reaction kinetics in porous media: An experimental pore scale quantification. Environmental science & technology 2013;48(1):508–516.

Archie, G.. The electrical resistivity log as an aid in determining some reservoir characteristics. Transaction of the american institute of mining and metallurgical engineers 1942;146:54–61.

Arènes, A., Latour, B., Gaillardet, J.. Giving depth to the surface: An exercise in the gaia-graphy of critical zones. The Anthropocene Review 2018;5(2):120–135.

Atekwana, E.A., Atekwana, E.A.. Geophysical signatures of microbial activity at hydrocarbon contaminated sites: a review. Surveys in Geophysics 2010;31(2):247–283.

Atekwana, E.A., Slater, L.D.. Biogeophysics: A new frontier in earth science research. Reviews of Geophysics 2009;47(4).

Bear, J.. Dynamics of Fluids in Porous Media. New York: Dover Publications, 1988. 784 pages.

Binley, A., Cassiani, G., Middleton, R., Winship, P.. Vadose zone flow model parameterisation using cross-borehole radar and resistivity imaging. Journal of Hydrology 2002;267(3):147–159.

Binley, A., Hubbard, S.S., Huisman, J.A., Revil, A., Robinson, D.A., Singha, K., Slater, L.D.. The emergence of hydrogeophysics for improved understanding of subsurface processes over multiple scales. Water resources research 2015;51(6):3837–3866.

Binley, A., Kemna, A.. Dc resistivity and induced polarization methods. In: Hydrogeophysics. Springer; 2005. p. 129–156.

Bordes, C., Sénéchal, P., Barrière, J., Brito, D., Normandin, E., Jougnot, D.. Impact of water saturation on seismoelectric transfer functions: a laboratory study of coseismic phenomenon. Geophysical Journal International 2015;200(3):1317–1335.

Borgne, T.L., Ginn, T.R., Dentz, M.. Impact of fluid deformation on mixing-induced chemical reactions in heterogeneous flows. Geophysical Research Letters 2014;41(22):7898–7906.

Briggs, M.A., Day-Lewis, F.D., Ong, J.B., Harvey, J.W., Lane, J.W.. Dual-domain mass-transfer parameters from electrical hysteresis: Theory and analytical approach applied to laboratory, synthetic streambed, and groundwater experiments. Water Resources Research 2014;50(10):8281–8299.

Carsel, R.F., Parrish, R.S.. Developing joint probability distributions of soil water retention characteristics. Water resources research 1988;24(5):755–769.

Chorover, J., Kretzschmar, R., Garcia-Pichel, F., Sparks, D.L.. Soil biogeochemical processes within the critical zone. Elements 2007;3(5):321–326.

Clair, J.S., Moon, S., Holbrook, W., Perron, J., Riebe, C., Martel, S., Carr, B., Harman, C., Singha, K., Richter, D.d.. Geophysical imaging reveals topographic stress control of bedrock weathering. Science 2015;350(6260):534–538.

Dangeard, M., Bodet, L., Pasquet, S., Thiesson, J., Guérin, R., Jougnot, D., Longuevergne, L.. Estimating picking errors in near-surface seismic data to enable their time-lapse interpretation of hydrosystems. Near Surface Geophysics 2018;16(6):613–625.

Darnet, M., Marquis, G.. Modelling streaming potential (sp) signals induced by water movement in the vadose zone. Journal of hydrology 2004;285(1-4):114–124.

Davis, C.A., Pyrak-Nolte, L.J., Atekwana, E.A., Werkema Jr, D.D., Haugen, M.E.. Acoustic and electrical property changes due to microbial growth and biofilm formation in porous media. Journal of Geophysical Research: Biogeosciences 2010;115(G3).

Day-Lewis, F., Linde, N., Haggerty, R., Singha, K., Briggs, M.A.. Pore network modeling of the electrical signature of solute transport in dual-domain media. Geophysical Research Letters 2017;44(10):4908–4916.

Day-Lewis, F.D., Singha, K., Binley, A.M.. Applying petrophysical models to radar travel time and electrical resistivity tomograms: Resolution-dependent limitations. Journal of Geophysical Research: Solid Earth 2005;110(B8).

DesRoches, A.J., Butler, K.E., MacQuarrie, K.T.. Surface self-potential patterns related to transmissive fracture trends during a water injection test. Geophysical Journal International 2017;212(3):2047–2060.

Doussan, C., Jouniaux, L., Thony, J.. Variations of self-potential and unsaturated water flow with time in sandy loam and clay loam soils. Journal of Hydrology 2002;267(3):173–185.

Fagerlund, F., Heinson, G.. Detecting subsurface groundwater flow in fractured rock using self-potential (sp) methods. Environmental Geology 2003;43(7):782–794.

Flemming, H.C., Wingender, J., Szewzyk, U., Steinberg, P., Rice, S.A., Kjelleberg, S.. Biofilms: an emergent form of bacterial life. Nature Reviews Microbiology 2016;14(9):563.

Fox, R.W.. On the electromagnetic properties of metalliferous veins in the mines of cornwall. Philosophical Transactions of the Royal Society 1830;120:399–414.

Frenkel, J.. On the theory of seismic and seismoelectric phenomena in a moist soil. Journal of Physics 1944;III(4):230–241.

Gaillardet, J., Braud, I., Hankard, F., Anquetin, S., Bour, O., Dorfliger, N., De Dreuzy, J.R., Galle, S., Galy, C., Gogo, S., et al. Ozcar: The french network of critical zone observatories. Vadose Zone Journal 2018;17(1).

Gélis, C., Revil, A., Cushing, M., Jougnot, D., Lemeille, F., Cabrera, J., De Hoyos, A., Rocher, M.. Potential of electrical resistivity tomography to detect fault zones in limestone and argillaceous formations in the experimental platform of tournemire, france. Pure and Applied Geophysics 2010;167(11):1405–1418.

Ghorbani, A.. Contribution au développement de la résistivité complexe et à ses applications en environnement. Mémoire de thèse de doctorat Université Pierre-et-Marie-Curie, Paris (France) 2007;.

Ghorbani, A., Cosenza, P., Revil, A., Zamora, M., Schmutz, M., Florsch, N., Jougnot, D.. Non-invasive monitoring of water content and textural changes in clay-rocks using spectral induced polarization: A laboratory investigation. Applied Clay Science 2009;43(3-4):493–502.

Ghosh, U., Borgne, T., Jougnot, D., Linde, N., Méheust, Y.. Geoelectrical signatures of reactive mixing: a theoretical assessment. Geophysical Research Letters 2018;45(8):3489–3498.

Gibert, D., Nicollin, F., Kergosien, B., Bossart, P., Nussbaum, C., Grislin-Mouëzy, A., Conil, F., Hoteit, N.. Electrical tomography monitoring of the excavation damaged zone of the gallery 04 in the mont terri rock laboratory: Field experiments, modelling, and relationship with structural geology. Applied clay science 2006;33(1):21–34.

Glover, P.. Geophysical properties of the near surface earth: electrical properties. Treatise on Geophysics 2015;11:89–137.

Guarracino, L., Jougnot, D.. A physically based analytical model to describe effective excess charge for streaming potential generation in water saturated porous media. Journal of Geophysical Research: Solid Earth 2018;123(1):52–65.

Heberling, F., Vinograd, V.L., Polly, R., Gale, J.D., Heck, S., Rothe, J., Bosbach, D., Geckeis, H., Winkler, B.. A thermodynamic adsorption/entrapment model for selenium (iv) coprecipitation with calcite. Geochimica et Cosmochimica Acta 2014;134:16–38.

Helmholtz, H.V.. Studien über electrische grenzschichten. Annalen der Physik 1879;243(7):337–382.

Holzhauer, J., Yaramanci, U.. Improvements in seismoelectric acquisitions at field and lab scales and records interpretation. In: Near Surface 2011-17th EAGE European Meeting of Environmental and Engineering Geophysics. 2011. .

Hubbard, S., Linde, N.. Hydrogeophysics. In: Wilderer, P., editor. Treatise on Water Science. Oxford: Academic Press; volume 1; 2011. p. 401–434.

Hunter, R.. Zeta Potential in Colloid Science: Principles and Applications. Colloid Science Series. Academic Press, 1981.

Jackson, M.D.. Characterization of multiphase electrokinetic coupling using a bundle of capillary tubes model. Journal of Geophysical Research 2008;113(B4).

Jackson, M.D.. Multiphase electrokinetic coupling: Insights into the impact of fluid and charge distribution at the pore scale from a bundle of capillary tubes model. Journal of Geophysical Research 2010;115.

Jardani, A., Revil, A., Dupont, J.P.. Stochastic joint inversion of hydrogeophysical data for salt tracer test monitoring and hydraulic conductivity imaging. Advances in water resources 2013;52:62–77.

Jiménez-Martínez, J., Anna, P.d., Tabuteau, H., Turuban, R., Borgne, T.L., Méheust, Y.. Pore-scale mechanisms for the enhancement of mixing in unsaturated porous media and implications for chemical reactions. Geophysical Research Letters 2015;42(13):5316–5324.

Jougnot, D.. New approach to up-scale the frequency-dependent effective excess charge density for seismoelectric modeling. In: SEG Technical Program Expanded Abstracts 2019. 2019. p. 3608–3612.

Jougnot, D., Ghorbani, A., Revil, A., Leroy, P., Cosenza, P.. Spectral induced polarization of partially saturated clay-rocks: A mechanistic approach. Geophysical Journal International 2010a;180(1):210–224.

Jougnot, D., Jiménez-Martínez, J., Legendre, R., Le Borgne, T., Méheust, Y., Linde, N.. Impact of small-scale saline tracer heterogeneity on electrical resistivity monitoring in fully and partially saturated porous media: insights from geoelectrical milli-fluidic experiments. Advances in water resources 2018;113:295–309.

Jougnot, D., Lewandowska, J., Gotteland, P., Revil, A.. Hydraulic conductivity of unsaturated double porosity geomaterials. In: Proc. of the 11th Baltic Sea Geotechnical Conference" Geotechnics in maritime engineering. 2008. p. 867–874.

Jougnot, D., Linde, N.. Self-potentials in partially saturated media: the importance of explicit modeling of electrode effects. Vadose Zone Journal 2013;12(2).

Jougnot, D., Linde, N., Haarder, E.B., Looms, M.C.. Monitoring of saline tracer movement with vertically distributed self-potential measurements at the hobe agricultural test site, voulund, denmark. Journal of Hydrology 2015;521:314–327.

Jougnot, D., Linde, N., Revil, A., Doussan, C.. Derivation of soil-specific streaming potential electrical parameters from hydrodynamic characteristics of partially saturated soils. Vadose Zone Journal 2012;11(1).

Jougnot, D., Mendieta, A., Leroy, P., Maineult, A.. Exploring the effect of the pore size distribution on the streaming potential generation in saturated porous media, insight from pore network simulations. Journal of Geophysical Research: Solid Earth 2019;124(6):5315–5335.

Jougnot, D., Revil, A.. Thermal conductivity of unsaturated clay-rocks. Hydrology and Earth System Sciences 2010;14(1):91–98.

Jougnot, D., Revil, A., Leroy, P.. Diffusion of ionic tracers in the callovo-oxfordian clay-rock using the donnan equilibrium model and the formation factor. Geochimica et Cosmochimica Acta 2009;73(10):2712–2726.

Jougnot, D., Revil, A., Lu, N., Wayllace, A.. Transport properties of the callovo-oxfordian clay rock under partially saturated conditions. Water Resources Research 2010b;46(8):W08514.

Jougnot, D., Roubinet, D., Guarracino, L., Maineult, A.. Modeling streaming potential in porous and fractured media, description and benefits of the effective excess charge density approach. In: Advances in Modeling and Interpretation in Near Surface Geophysics. Springer; 2020. p. 61–96.

Jougnot, D., Rubino, J.G., Rosas-Carbajal, M., Linde, N., Holliger, K.. Seismoelectric effects due to mesoscopic heterogeneities. Geophysical Research Letters 2013;40(10):2033–2037.

Jouniaux, L., Maineult, A., Naudet, V., Pessel, M., Sailhac, P.. Review of self-potential methods in hydrogeophysics. Comptes Rendus Geosciences 2009;341(10-11):928–936.

Jouniaux, L., Zyserman, F.. A review on electrokinetically induced seismo-electrics, electro-seismics, and seismo-magnetics for earth sciences. Solid Earth 2016;7(1):249.

Leinov, E., Jackson, M.D.. Experimental measurements of the SP response to concentration and temperature gradients in sandstones with application to subsurface geophysical monitoring. Journal of Geophysical Research–Solid Earth 2014;119.

Leroy, P., Jougnot, D., Revil, A., Lassin, A., Azaroual, M.. A double layer model of the gas bubble/water interface. Journal of Colloid and Interface Science 2012;388(1):243–256.

Leroy, P., Li, S., Jougnot, D., Revil, A., Wu, Y.. Modelling the evolution of complex conductivity during calcite precipitation on glass beads. Geophysical Journal International 2017;209(1):123–140.

Leroy, P., Revil, A.. A triple-layer model of the surface electrochemical properties of clay minerals. Journal of Colloid and Interface Science 2004;270(2):371–380.

Li, S., Leroy, P., Heberling, F., Devau, N., Jougnot, D., Chiaberge, C.. Influence of surface conductivity on the apparent zeta potential of calcite. Journal of colloid and interface science 2016;468:262–275.

Linde, N.. Comment on "characterization of multiphase electrokinetic coupling using a bundle of capillary tubes model" by mathew d. jackson. Journal of Geophysical Research 2009;114(B6):B06209.

Linde, N., Jougnot, D., Revil, A., Matthäi, S., Arora, T., Renard, D., Doussan, C.. Streaming current generation in two-phase flow conditions. Geophysical Research Letters 2007;34(3):L03306.

Lyklema, J., Dukhin, S., Shilov, V.. The relaxation of the double layer around colloidal particles and the low-frequency dielectric dispersion: Part i. theoretical considerations. Journal of Electroanalytical Chemistry and Interfacial Electrochemistry 1983;143(1-2):1–21.

Mahardika, H., Revil, A., Jardani, A.. Waveform joint inversion of seismograms and electrograms for moment tensor characterization of fracking events. Geophysics 2012;77(5):ID23–ID39.

Maldelbrot, B.B.. The fractal geometry of Nature. New York: W. H. Freeman and Company, 1983.

Mares, R., Barnard, H.R., Mao, D., Revil, A., Singha, K.. Examining diel patterns of soil and xylem moisture using electrical resistivity imaging. Journal of hydrology 2016;536:327–338.

Mewafy, F., Atekwana, E., Werkema Jr, D., Slater, L., Ntarlagiannis, D., Revil, A., Skold, M., Delin, G.. Magnetic susceptibility as a proxy for investigating microbially mediated iron reduction. Geophysical Research Letters 2011;38(21):L21402.

Monachesi, L.B., Rubino, J.G., Rosas-Carbajal, M., Jougnot, D., Linde, N., Quintal, B., Holliger, K.. An analytical study of seismoelectric signals produced by 1-d mesoscopic heterogeneities. Geophysical Journal International 2015;201(1):329–342.

Müller, T., Gurevich, B., Lebedev, M.. Seismic wave attenuation and dispersion resulting from wave-induced flow in porous rocks - A review. Geophysics 2010;75:A147–A164.

NRC, . Basic research opportunities in earth sciences. In: National Academy. 2001. .

Parsekian, A., Singha, K., Minsley, B.J., Holbrook, W.S., Slater, L.. Multiscale geophysical imaging of the critical zone. Reviews of Geophysics 2015;53(1):1–26.

Pasquet, S., Bodet, L.. Swip: An integrated workflow for surface-wave dispersion inversion and profilingsurface-wave inversion and profiling. Geophysics 2017;82(6):WB47–WB61.

Pasquet, S., Bodet, L., Bergamo, P., Guérin, R., Martin, R., Mourgues, R., Tournat, V.. Small-scale seismic monitoring of varying water levels in granular media. Vadose zone journal 2016;15(7).

Petiau, G.. Second generation of lead-lead chloride electrodes for geophysical applications. Pure and applied geophysics 2000;157(3):357–382.

Pollock, D., Cirpka, O.A.. Fully coupled hydrogeophysical inversion of a laboratory salt tracer experiment monitored by electrical resistivity tomography. Water Resources Research 2012;48(1).

Pride, S.. Governing equations for the coupled electromagnetics and accoustics of porous media. PHYSICAL REVIEW B 1994;50(21):15678–15696.

Pride, S., Garambois, S.. Electroseismic wave theory of Frenkel and more recent developments. JOURNAL OF ENGINEERING MECHANICS-ASCE 2005;131(9):898–907.

Quincke, G.. Ueber eine neue art elektrischer ströme. Annalen der Physik 1859;183(5):1–47.

Revil, A., Ahmed, A.S., Matthai, S.. Transport of water and ions in partially water-saturated porous media. part 3. electrical conductivity. Advances in water resources 2018;121:97–111.

Revil, A., Florsch, N.. Determination of permeability from spectral induced polarization in granular media. Geophysical Journal International 2010;181(3):1480–1498.

Revil, A., Jardani, A.. The Self-Potential Method: Theory and Applications in Environmental Geosciences. Cambridge University Press, 2013.

Revil, A., Jardani, A., Sava, P., Haas, A.. The Seismoelectric Method: Theory and Application. John Wiley & Sons, 2015.

Revil, A., Jougnot, D.. Diffusion of ions in unsaturated porous materials. Journal of colloid and interface science 2008;319(1):226–235.

Revil, A., Linde, N., Cerepi, A., Jougnot, D., Matthäi, S., Finsterle, S.. Electrokinetic coupling in unsaturated porous media. Journal of Colloid and Interface Science 2007;313(1):315–327.

Revil, A., Mendonça, C., Atekwana, E., Kulessa, B., Hubbard, S., Bohlen, K.. Understanding biogeobatteries: Where geophysics meets microbiology. Journal of Geophysical Research 2010;115(null):G00G02.

Rosas-Carbajal, M., Jougnot, D., Rubino, J.G., Monachesi, L.B., Linde, N., Holliger, K.. Seismoelectric exploration: Theory, experiments and applications; Wiley.

Roubinet, D., Irving, J.. Discrete-dual-porosity model for electric current flow in fractured rock. Journal of Geophysical Research: Solid Earth 2014;119(2):767–786.

Roubinet, D., Linde, N., Jougnot, D., Irving, J.. Streaming potential modeling in fractured rock: Insights into the identification of hydraulically active fractures. Geophysical Research Letters 2016;43(10):4937–4944.

Rubin, Y., Hubbard, S.S.. Hydrogeophysics. volume 50. Springer, 2005.

Rubino, J., Holliger, K.. Seismic attenuation and velocity dispersion in heterogeneous partially saturated porous rocks. Geophysical Journal International 2012;188:1088–1102.

Rubino, J., Ravazzoli, C., Santos, J.. Equivalent viscoelastic solids for heterogeneous fluid-saturated porous rocks. Geophysics 2009;74:N1–N13.

Rubino, J., Velis, D., Holliger, K.. Permeability effects on the seismic response of gas reservoirs. Geophys J Int 2012;189:448–468.

Rubino, J.G., Guarracino, L., Müller, T.M., Holliger, K.. Do seismic waves sense fracture connectivity? Geophys Res Lett 2013;.

Schlumberger, C.. Premières expériences. Carte des courbes équipotentielles, tracées au courant continu Val-Richer (Calvados) 1912;.

Schlumberger, C.. Etude sur la prospection electrique du sous-sol. paris 1920. Comptes Rendus, Paris 1920;170(519):21.

Singha, K., Day-Lewis, F.D., Lane Jr, J.W.. Geoelectrical evidence of bicontinuum transport in groundwater. Geophysical Research Letters 2007;34(12).

Singha, K., Gorelick, S.M.. Saline tracer visualized with three-dimensional electrical resistivity tomography: Field-scale spatial moment analysis. Water Resources Research 2005;41(5).

von Smoluchowski, M.. Contribution to the theory of electro-osmosis and related phenomena. Bull Int Acad Sci Cracovie 1903;3:184–199.

Soldi, M., Guarracino, L., Jougnot, D.. A simple hysteretic constitutive model for unsaturated flow. Transport in Porous Media 2017;120(2):271–285.

Soldi, M., Jougnot, D., Guarracino, L.. An analytical effective excess charge density model to predict the streaming potential generated by unsaturated flow. Geophysical Journal International 2019;216(1):380–394.

Thompson, R.. The seismic electric effect. Geophysics 1936;1(3):327–335.

Vereecken, H., Binley, A., Cassiani, G., Revil, A., Titov, K.. Applied hydrogeophysics. In: Applied Hydrogeophysics. Springer; 2006. p. 1–8.

Voytek, E.B., Barnard, H.R., Jougnot, D., Singha, K.. Transpiration-and precipitation-induced subsurface water flow observed using the self-potential method. Hydrological Processes 2019;.

Werkema Jr, D.D., Atekwana, E.A., Endres, A.L., Sauck, W.A., Cassidy, D.P.. Investigating the geoelectrical response of hydrocarbon contamination undergoing biodegradation. Geophysical Research Letters 2003;30(12).

Wishart, D.N., Slater, L.D., Gates, A.E.. Self potential improves characterization of hydraulically-active fractures from azimuthal geoelectrical measurements. Geophysical Research Letters 2006;33(17).

Wu, Y., Hubbard, S., Williams, K.H., Ajo-Franklin, J.. On the complex conductivity signatures of calcite precipitation. Journal of Geophysical Research: Biogeosciences 2010;115(G2).

Zisser, N., Kemna, A., Nover, G.. Relationship between low-frequency electrical properties and hydraulic permeability of low-permeability sandstones. Geophysics 2010;75(3):E131–E141.